OOF And Beyond: 2D Plasticity and 3D Microstructure-based Modeling

A. Ayyar[1] and N. Chawla[2]

[1]Department of Mechanical and Aerospace Engineering
[2]School of Materials
Fulton School of Engineering
Arizona State University
Tempe, AZ 85287-6006 USA

ARIZONA STATE UNIVERSITY

OOF Workshop - June, 2001

11:00 Myriad Uses
Craig Carter, M.I.T.
11:30 Discussion
11:45 3-D Meshing
Panos Charalambides, Univ. of Maryland Baltimore County
12:15 Discussion
12:30 - 13:45 Lunch - NIST cafeteria
Thursday Afternoon - PROJECT SESSION
A session for OOF users and potential users, discussing what they have done and/or what they would like to do.
13:45 OOF Research at Ford Research Lab
Alex Bogicevic, Ford Research Lab
14:00 Thermal Conductivity Simulations for TBC's
Jim Ruud, GE CRD
14:20 Microstructure-Properties Correlation for Thermal Spray TBC's
Matthias Oechsner, Siemens Westinghouse Power Corporation
14:30 Overview of OOF Research at ORNL
Chun-Hway Hsueh, Oak Ridge Nat'l Lab
14:40 Discussion
15:00 OOF Research in Polymers
Martin Chiang, Polymers, NIST
15:15 Piezoelectricity and Beyond
Edwin Garcia, M.I.T.
15:35 OIM-2-OOF code
Venkata Vedula, Sandia National Labs
15:45 Discussion
15:55 **Break**
16:10 Residual Stresses in Ceramics
Yi Fang, Univ. of Houston
16:25 Microcracking in Alumina/Aluminum Titanate
Susan Galal Yousef, TU-Darmstadt
16:35 Thermomechanical stresses in composites
Nik Chawla, Arizona State Univ.
16:50 Marcelling Effects on Layered Composite Deformation
Venkata Vedula, UTRC
16:55 Discussion
17:10 Zebulon: Object-Oriented, Finite Element Software for Material
Behavior Development, Alan C. Mueller, Northwest Numerics, Inc.
17:20 Elle: Microstructure Modelling of Geological Materials
Lynn Evans, Monash University
17:25 Thermal Degradation of Marble
Thomas Weiss, Georg August Universität
17:45 Discussion
18:00 to Dinner

Modeling efforts at ASU

2D Modeling
Elastic
OOF

OOF in Education

2D Modeling
Elastic-plastic
ABAQUS

2D Crack growth modeling
Elastic
FRANC2D/L

3D Visualization
Serial Sectioning
ImageJ, RasterVect, SurfDriver, Mimics

3D Modeling
Elastic-plastic
ABAQUS

3D Crack growth modeling
Elastic
FRANC3D

Modeling at multi-length scales

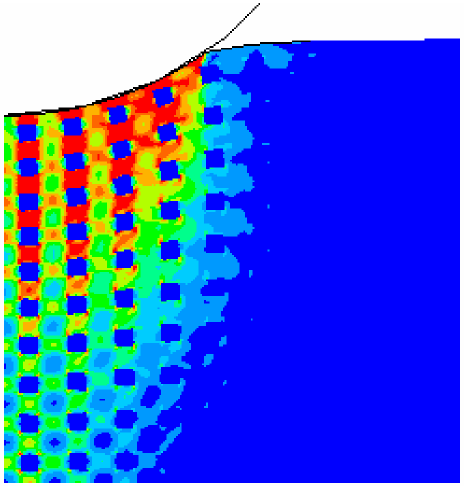

Continuum-based Modeling

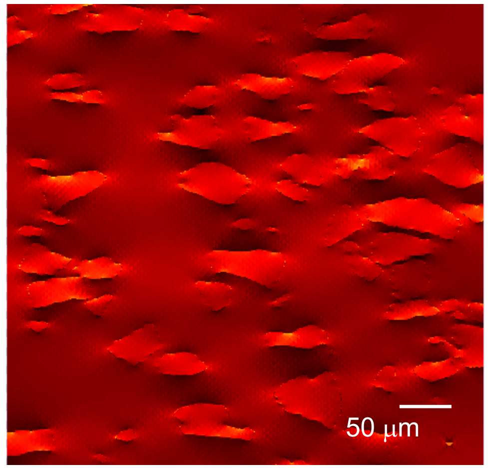

Microstructure-based Modeling

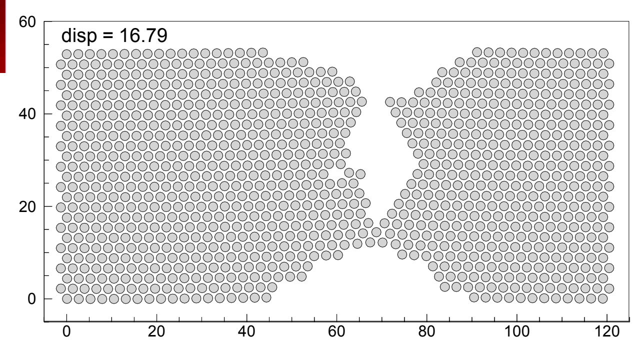

Dislocation-based Modeling

Atomistic Modeling

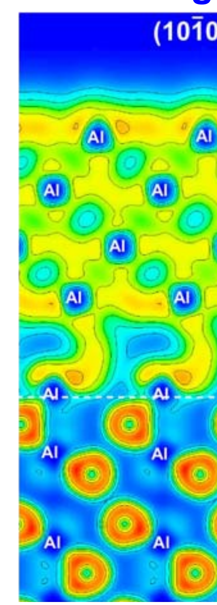

Decreasing Length scale

Microstructure of extruded particle reinforced aluminum

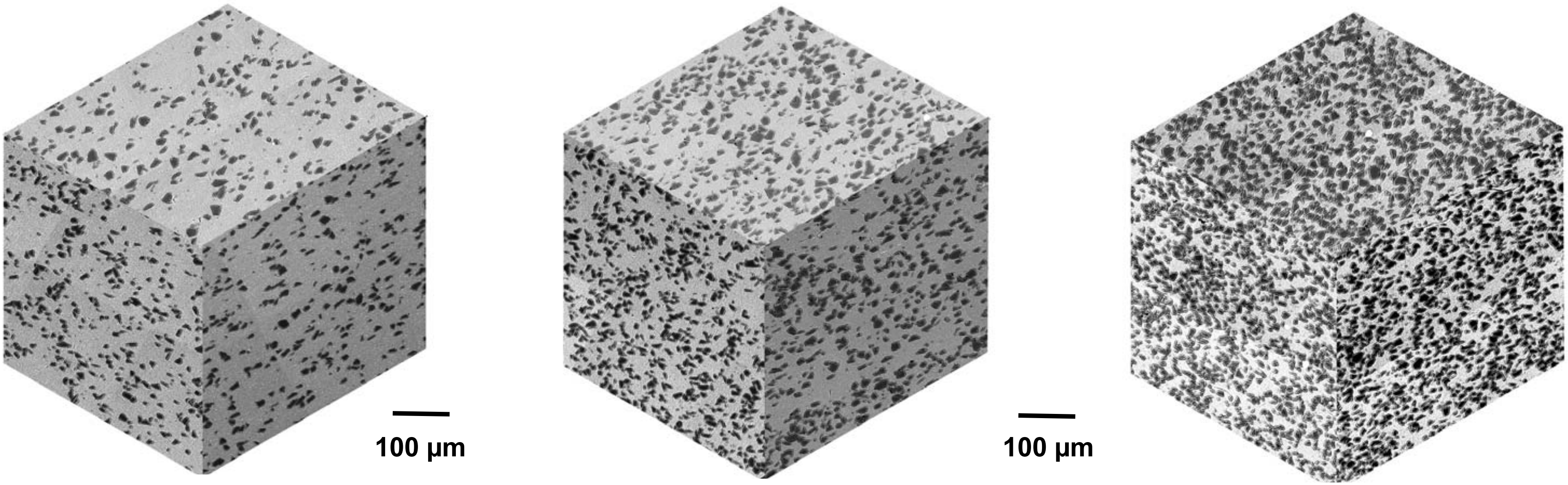

$2080/SiC/10_p$ F(600)

$2080/SiC/20_p$ F(600)

$2080/SiC/30_p$ F(600)

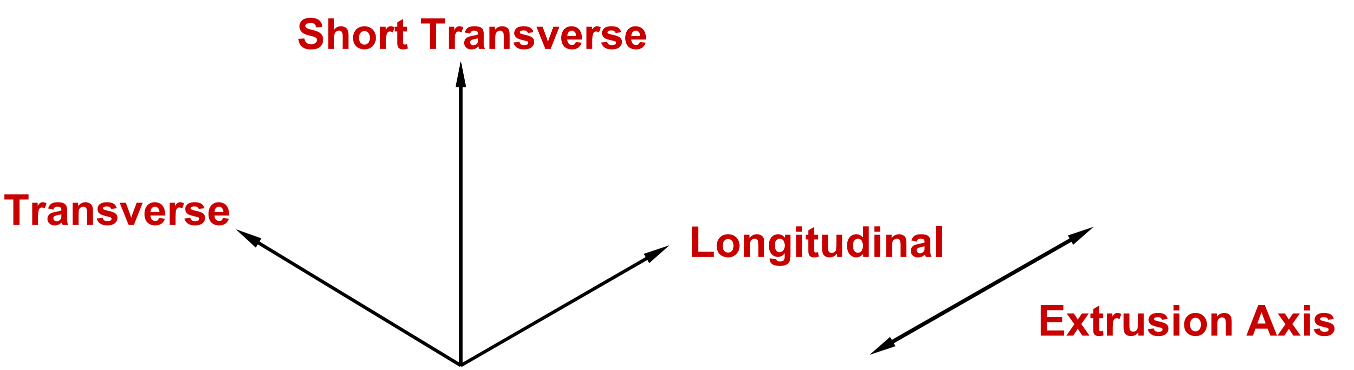

Applications of MMCs

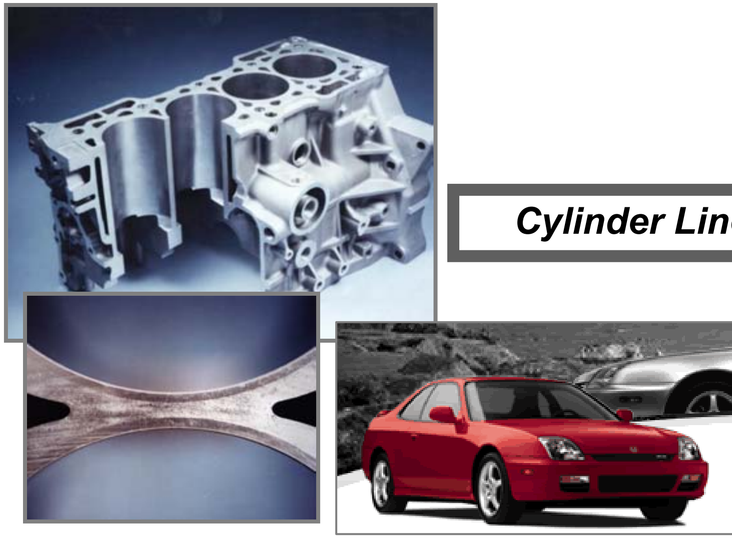

Cylinder Liners

MMC replaced gr/epoxy FEGV in PW 4XXX engines

Power conductors

MMC Spikes for Track and Field Cleats

N. Chawla and K.K. Chawla, Metal Matrix Composites, (2006), Springer.

Approaches to numerical modeling of composites

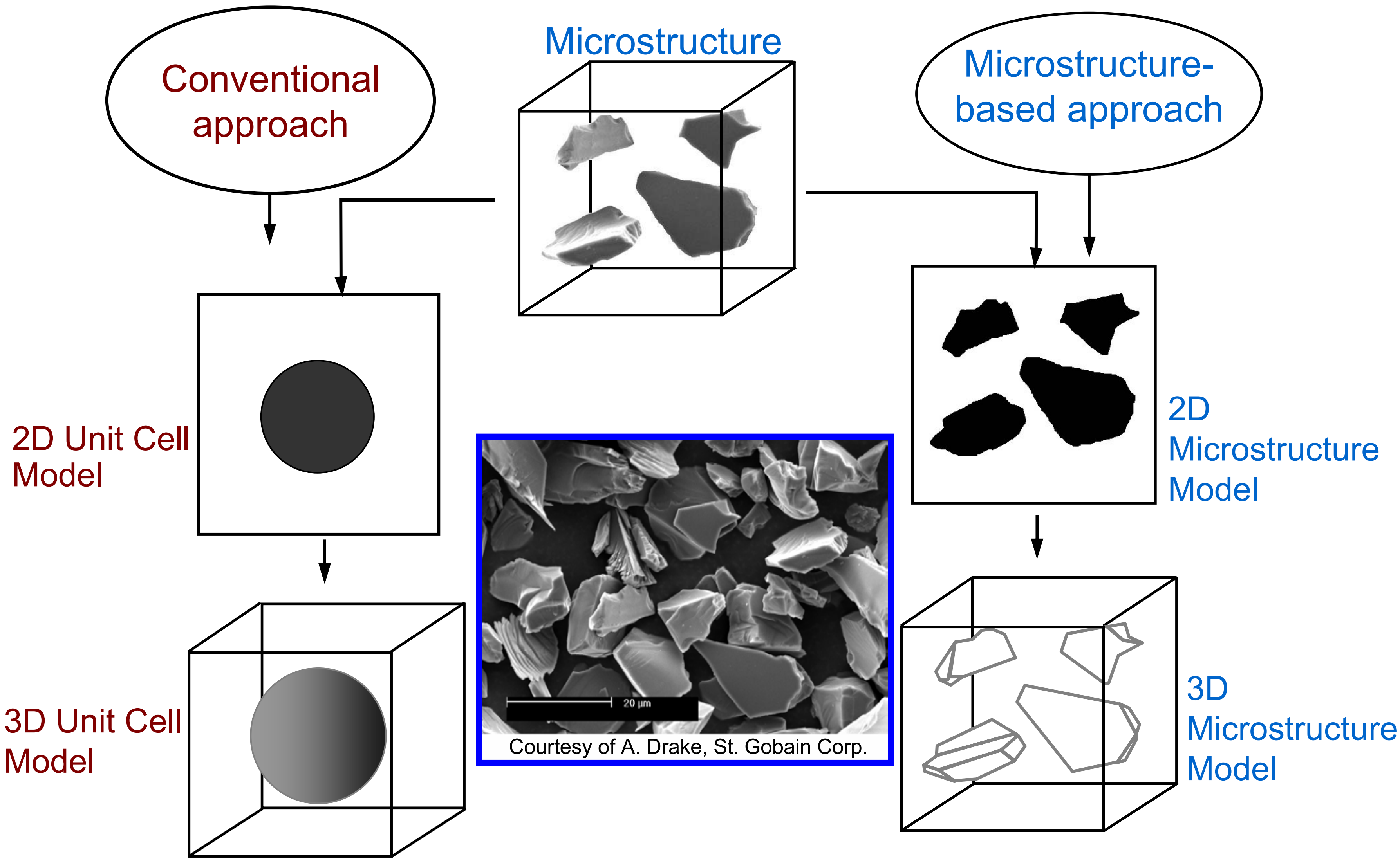

Modeling the effect of second phase morphology on Young's Modulus

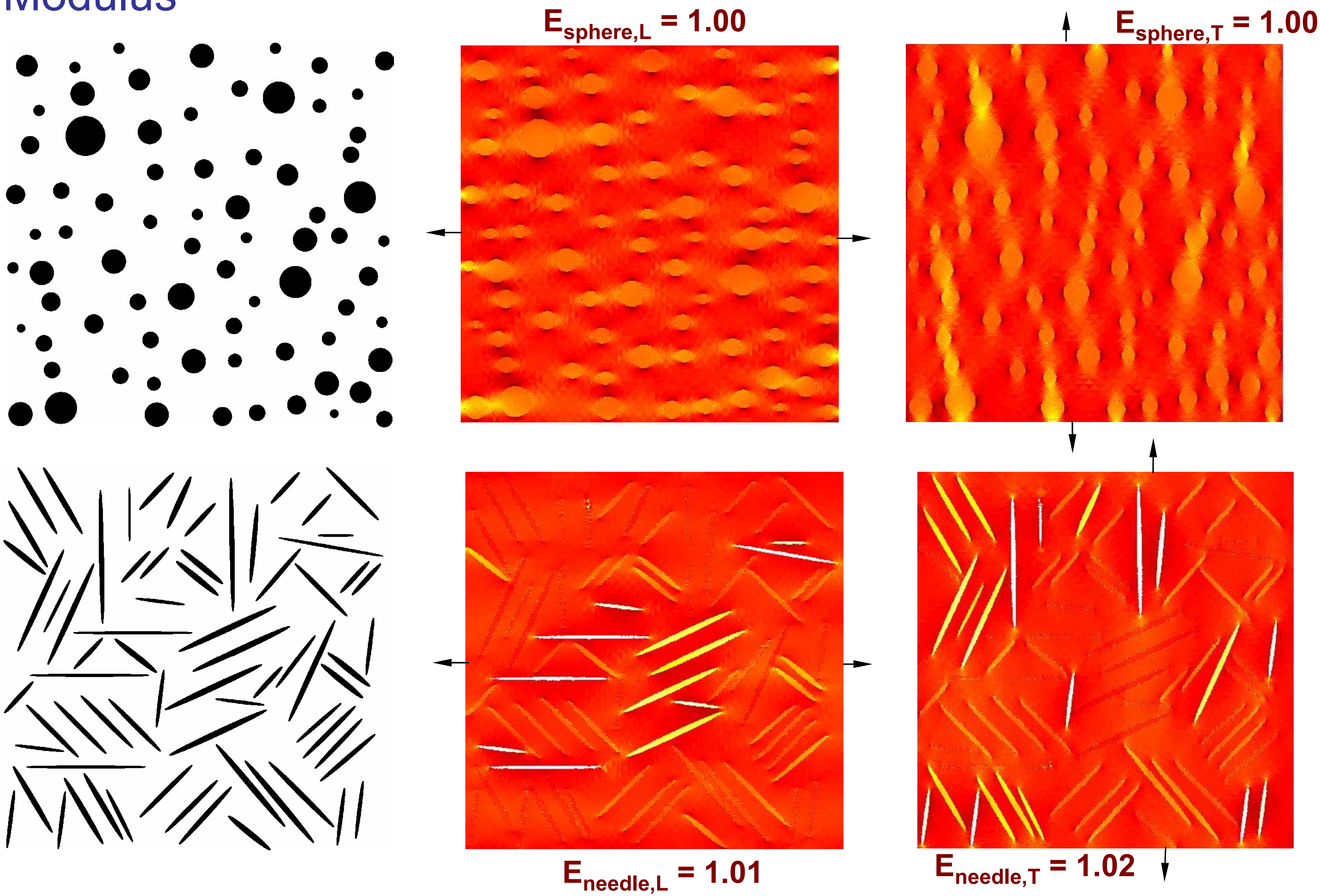

Chawla et al., J. Mater. Sci. – Mater. Elect., (2004).

2D Microstructure-based finite element analysis
Elastic analysis

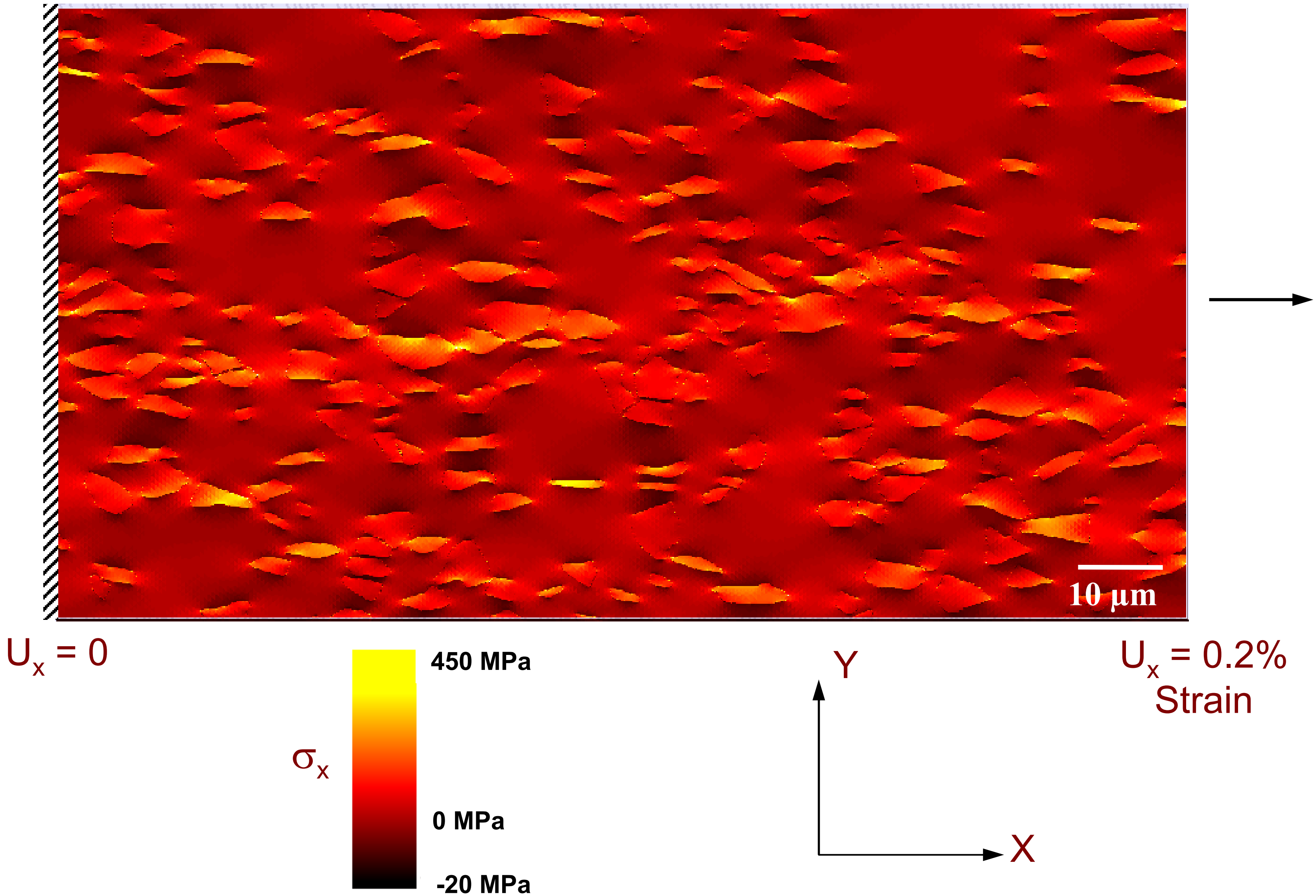

Chawla et al., Mater. Charac., (2003).

Stresses are inherently based on local microstructure characteristics – Elastic analysis

Particle free region, 82 MPa

Clustered region, 120 MPa

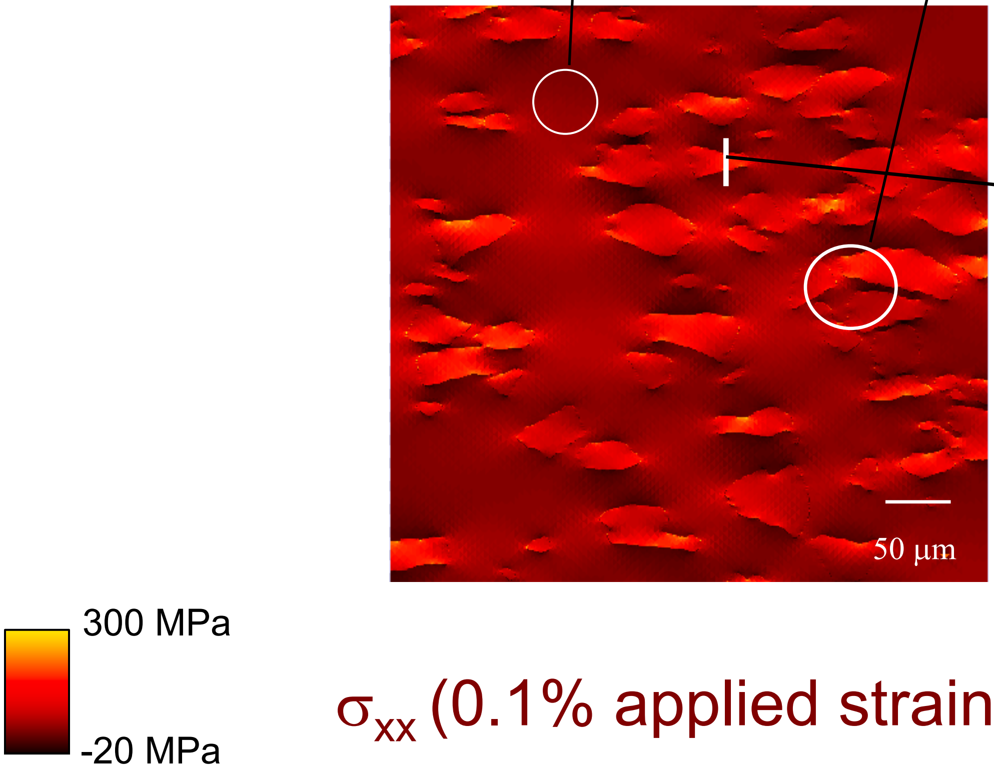

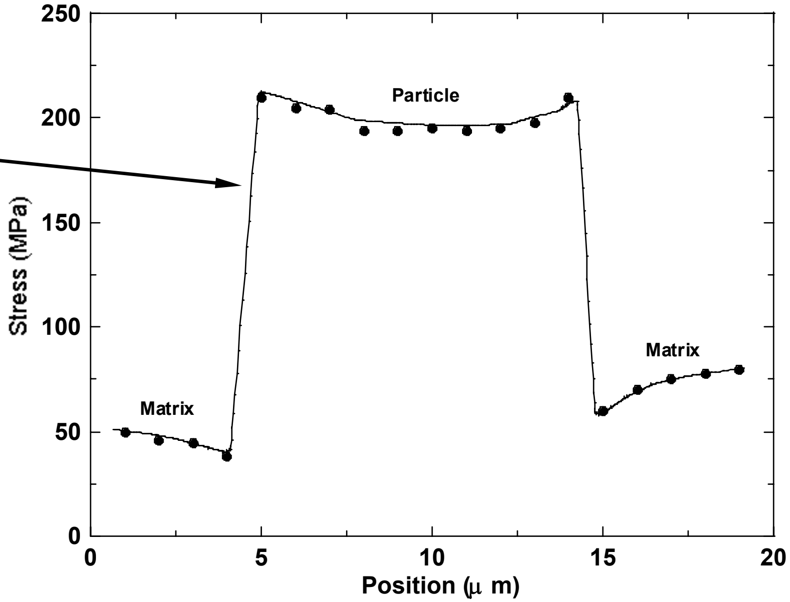

σ_{xx} (0.1% applied strain)

Chawla et al., Mater. Charac., (2003).

2D Microstructure-based modeling
Results of tensile anisotropy

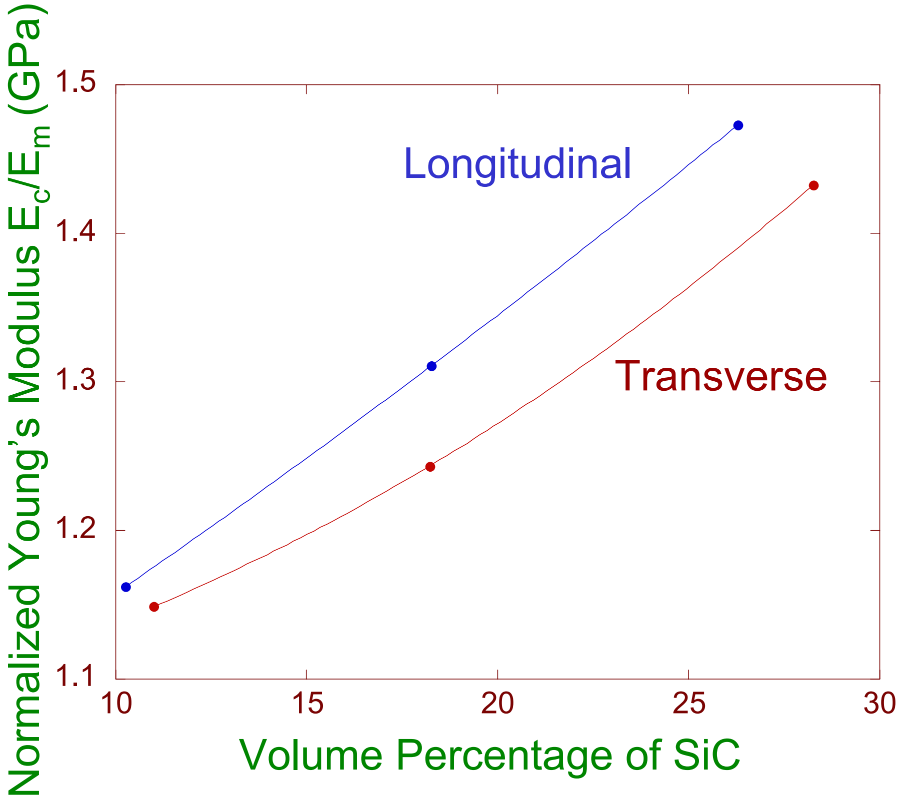

Microstructure based FEA was able to predict anisotropy in normalized Young's modulus

Thermal stress distribution

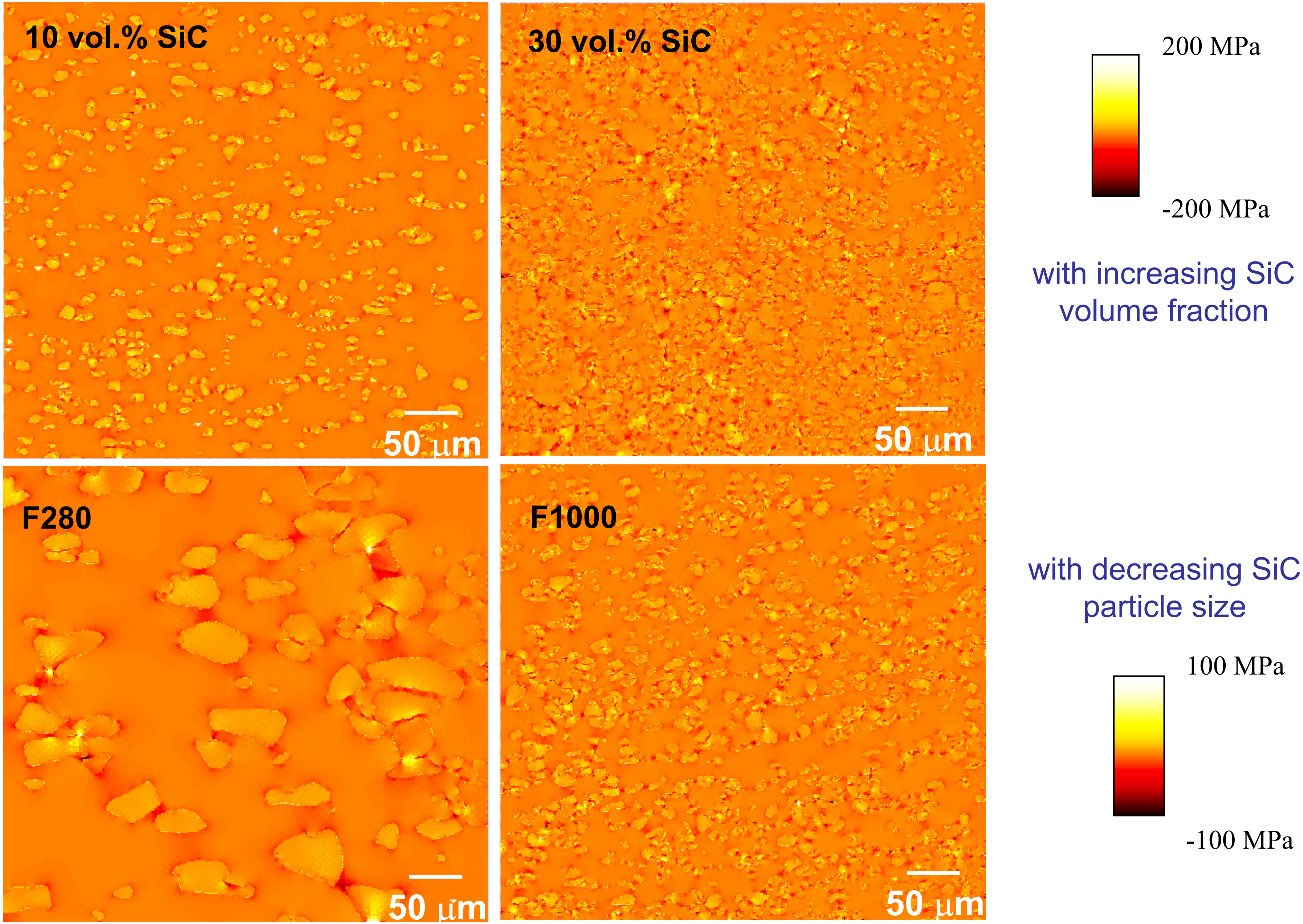

with increasing SiC volume fraction

with decreasing SiC particle size

Chawla et al., Mater. Charac., (2003).

Particle reinforced metal matrix composites

2080/SiC/10_p

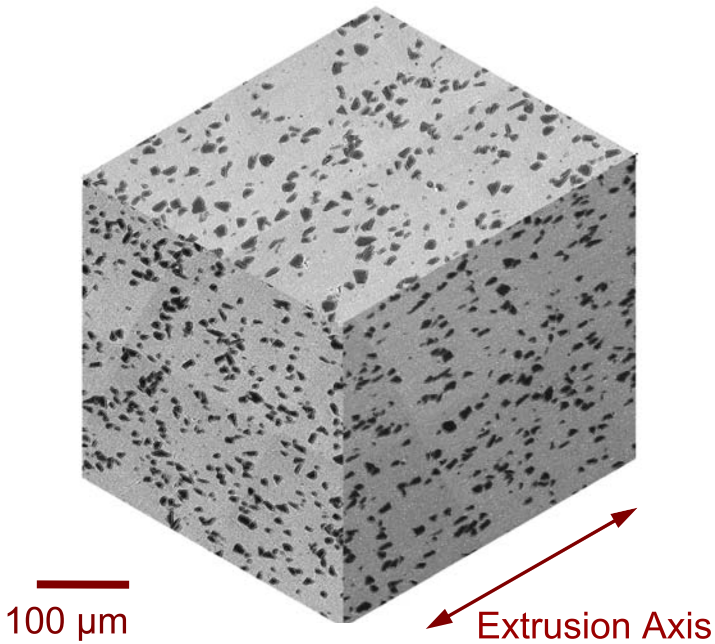

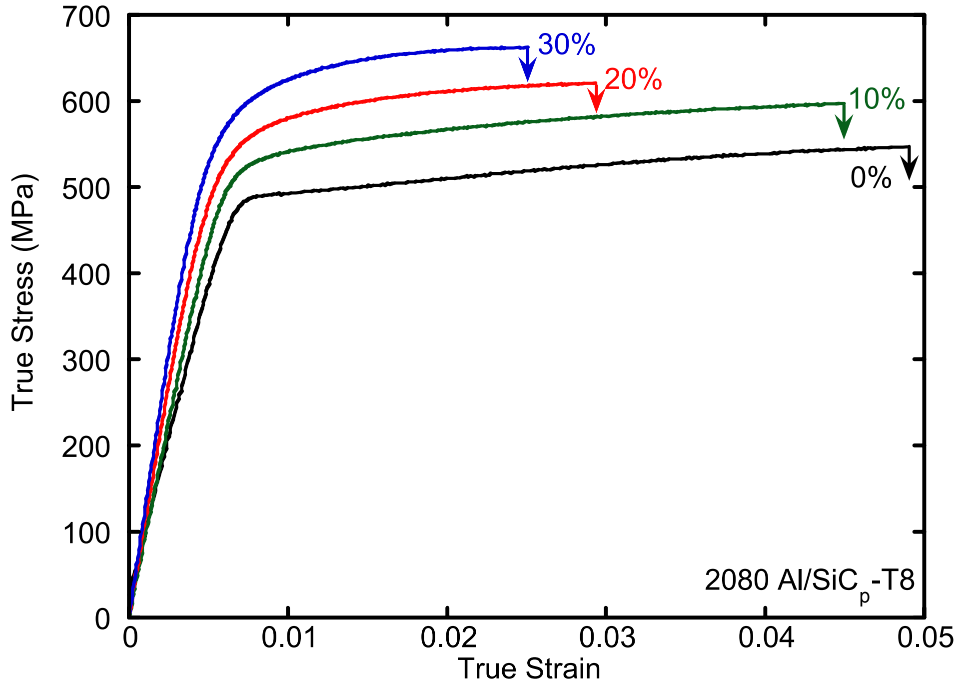

Ganesh and Chawla,
Metall. Mater. Trans. (2004)

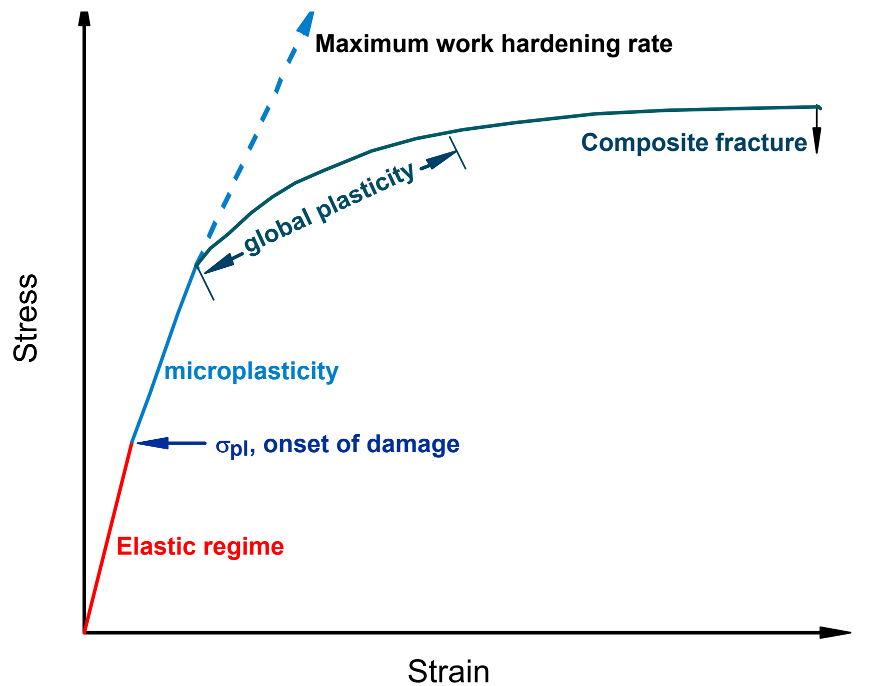

N. Chawla, C. Andres, J.W. Jones, J.E. Allison, Metall. Mater. Trans. (1998)

Variation of clustering in Al/SiC/15p

- Clustering was controlled by processing composites with varying Al:SiC particle size ratio
  - Blended, pressed and sintered
- Increasing the Al:SiC particle size ratio resulted in a greater degree of SiC clustering

Homogenous distribution

$D_{50}^{Al} = 7\mu m \quad D_{50}^{SiC} = 5\mu m$

Ratio = 1.4

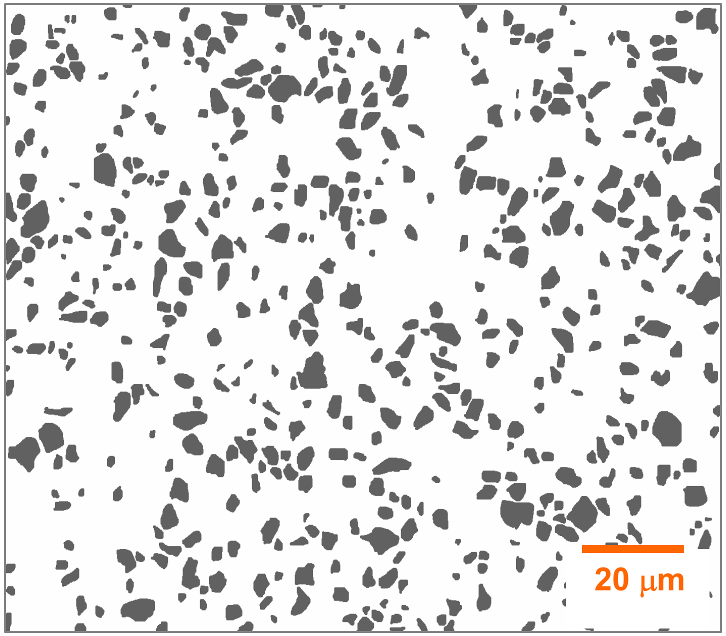

Clustered distribution

$D_{50}^{Al} = 33\mu m \quad D_{50}^{SiC} = 5\mu m$

Ratio = 6.6

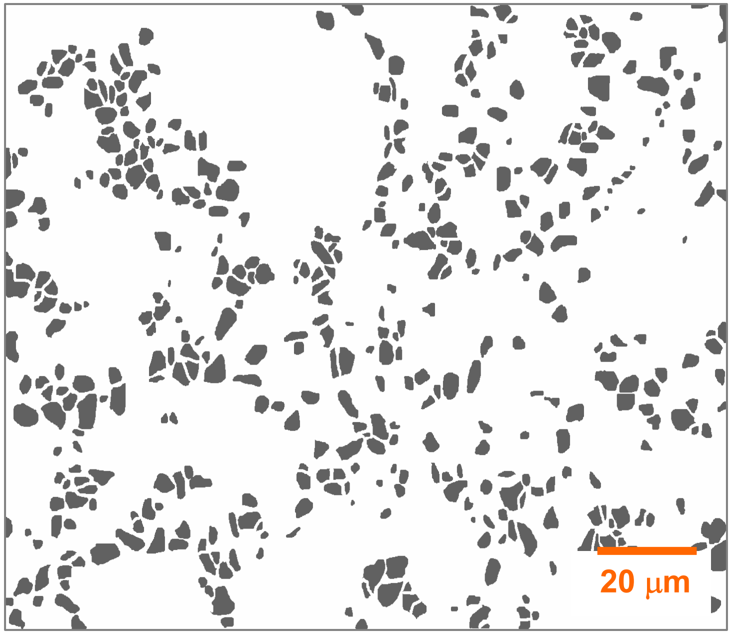

A. Ayyar and N. Chawla, *Comp. Sci. Tech.*, 66 (2006)

Processing by R. J. Fields, NIST

Incorporating actual microstructure into FEM

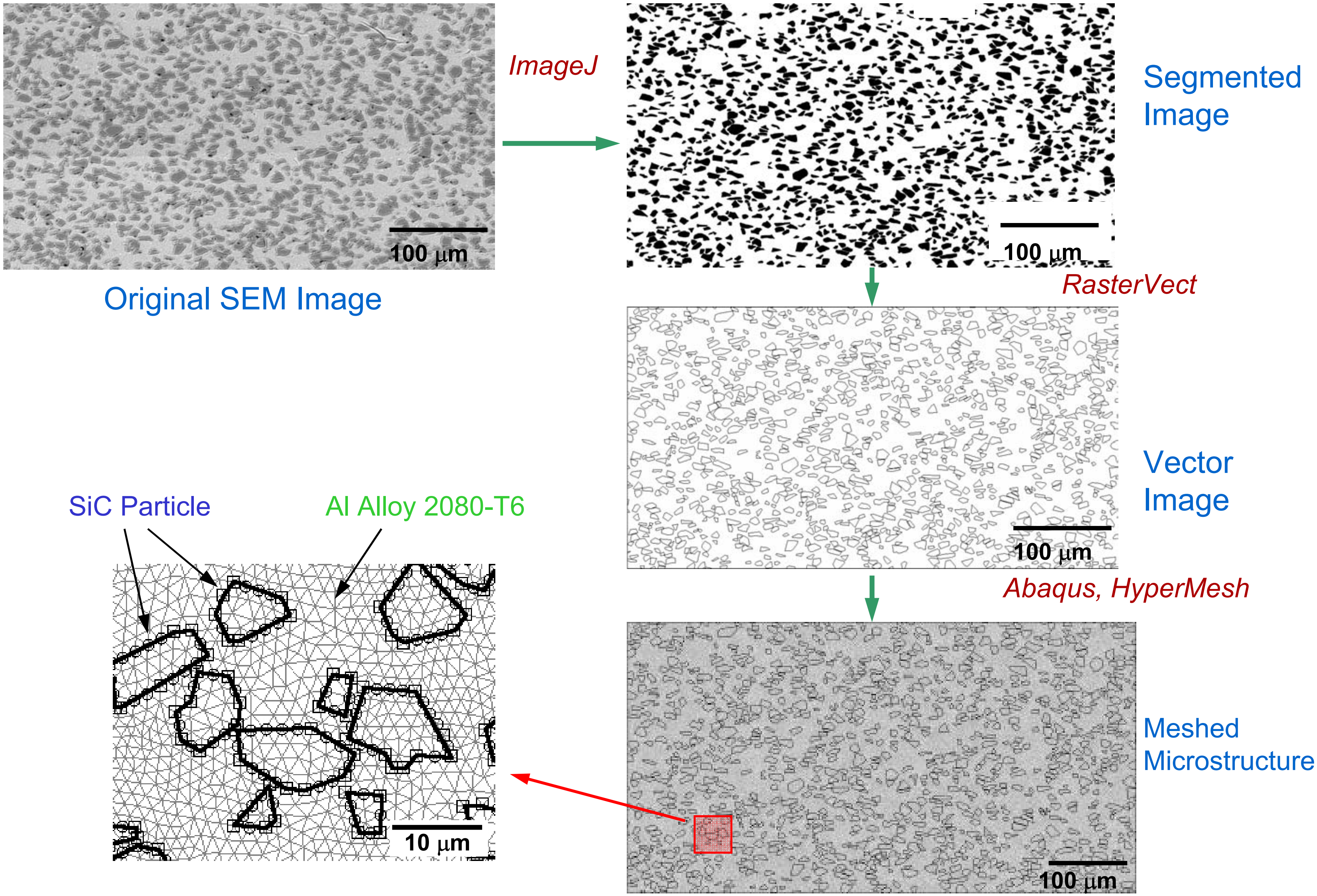

Effect of SiC particle clustering on local strain state

Elastic – plastic analysis

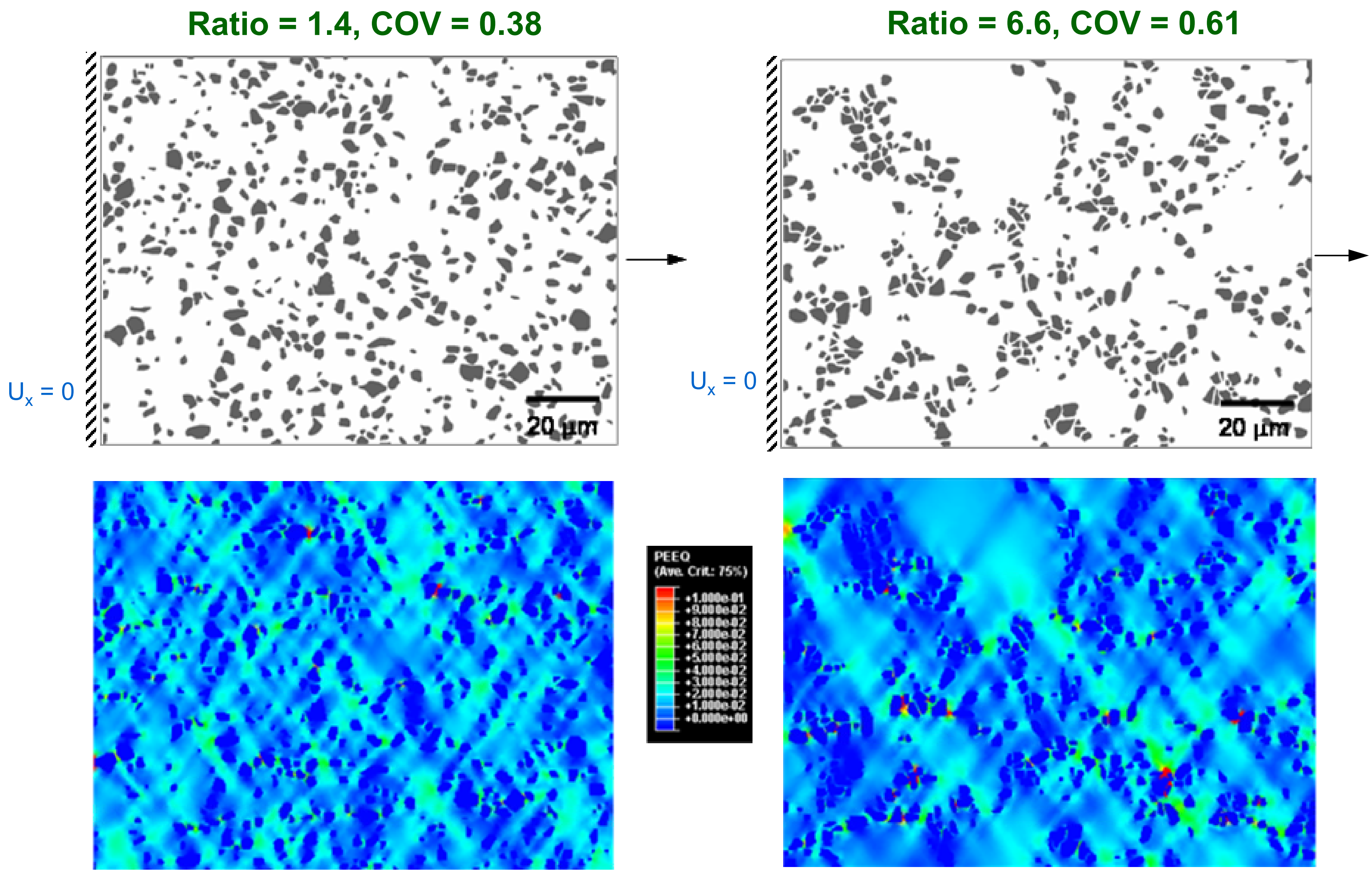

Need for 3D modeling

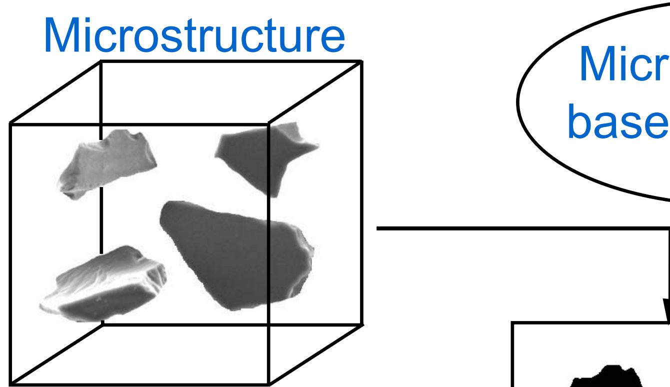

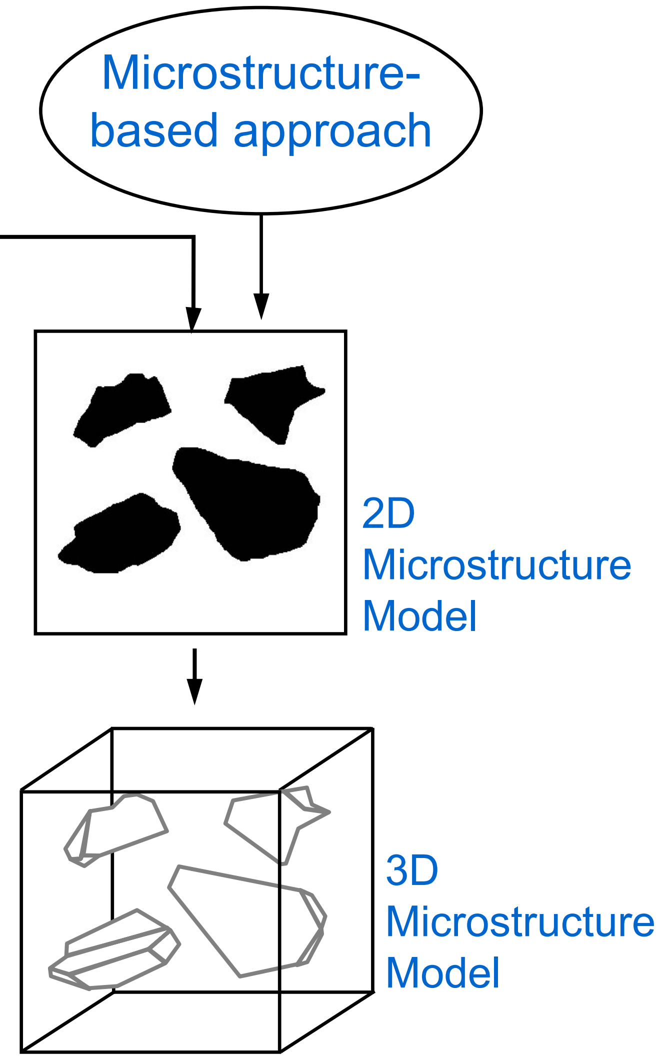

2D analysis is either plane stress or plane strain

SiC particles modeled as “discs” in 2D analysis

SiC particles have complex geometry

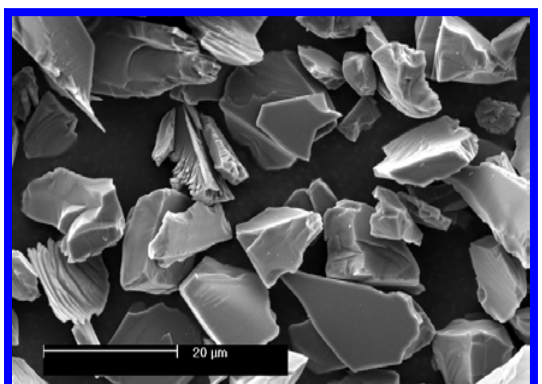

Courtesy of A. Drake, St. Gobain Corp.

Serial sectioning concept

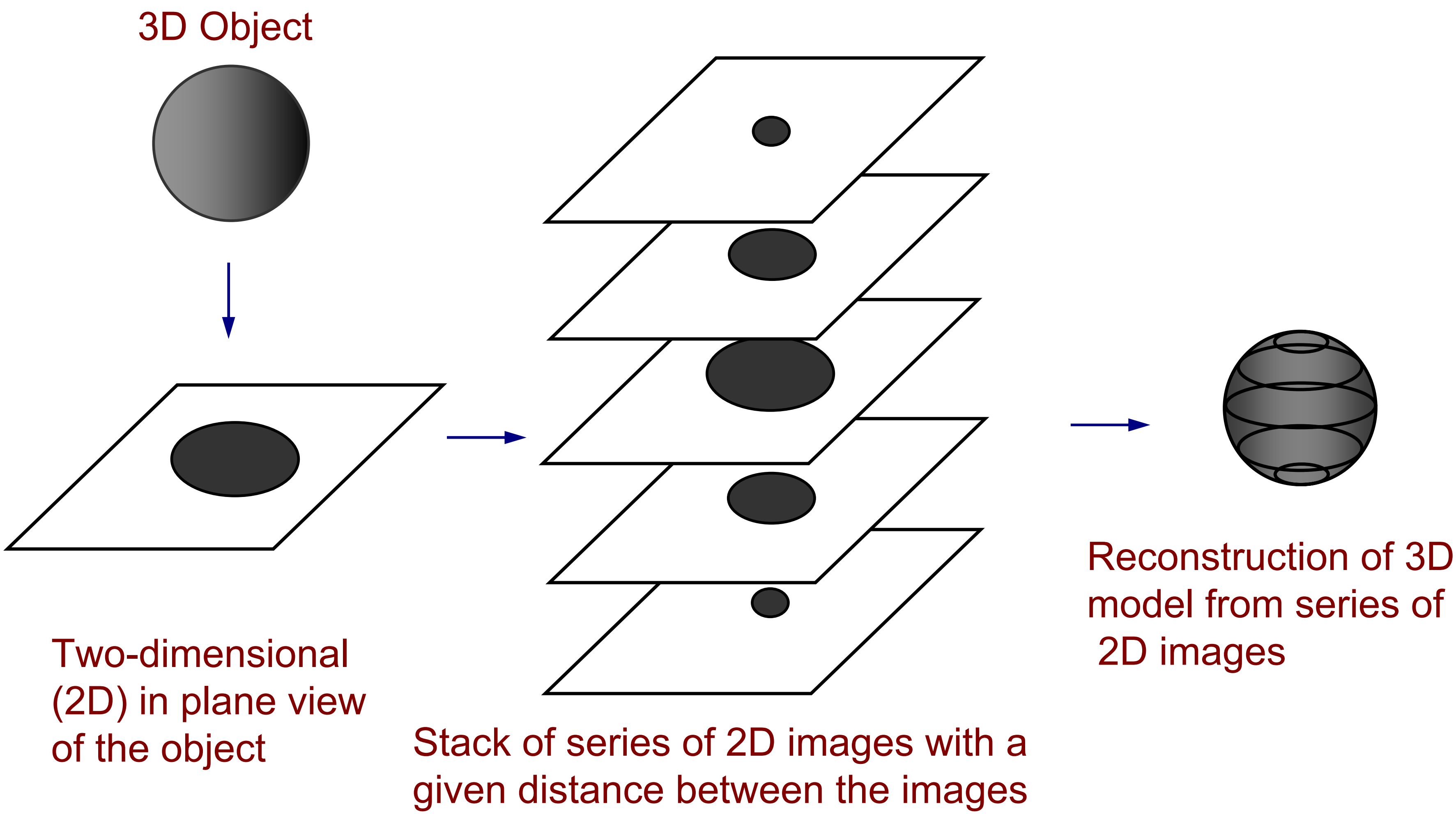

Serial sectioning process flow chart

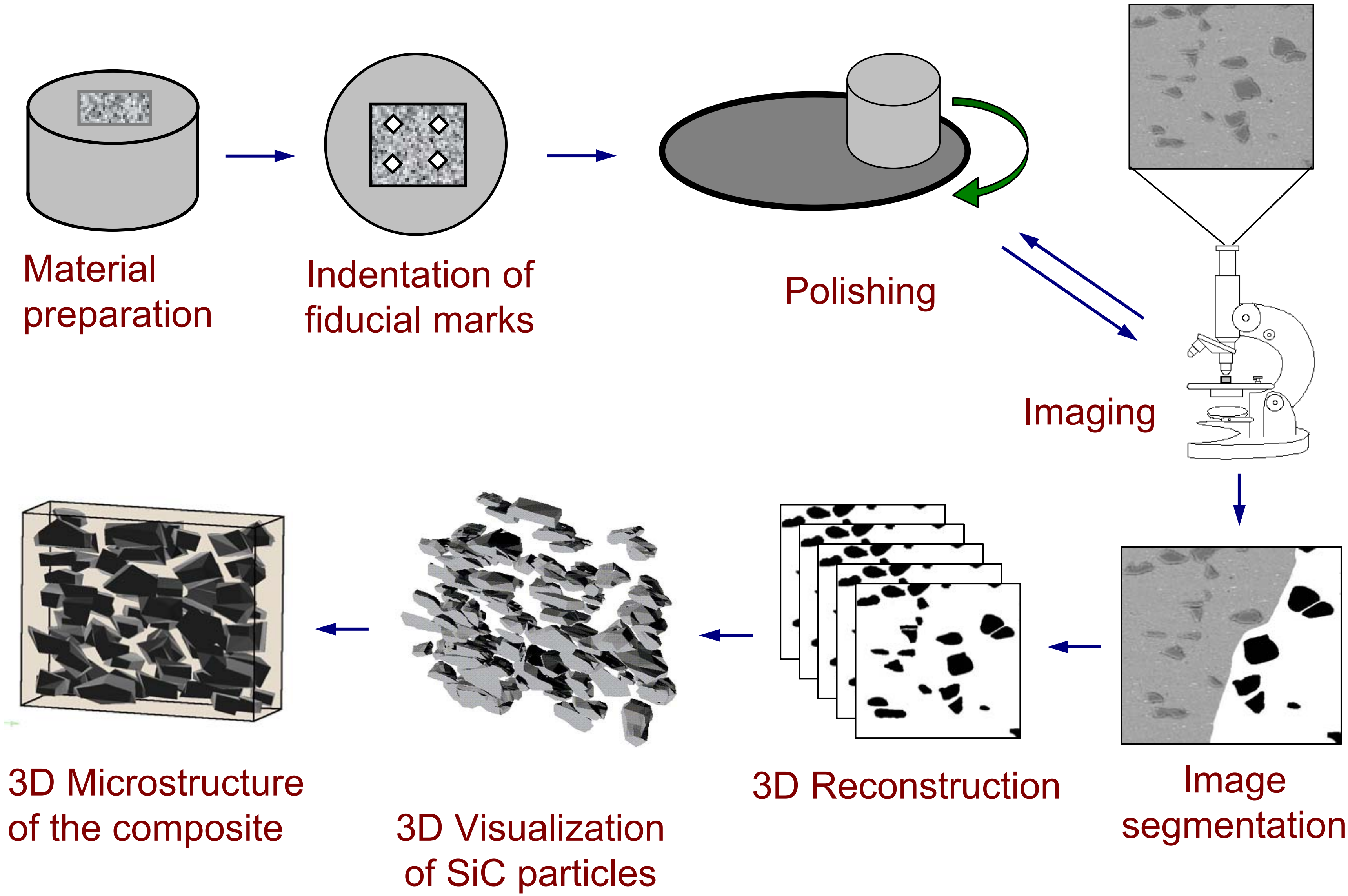

N. Chawla, V.V. Ganesh, B. Wunsch, *Scripta Mater*. (2004).

Serial sectioning process – Region of interest

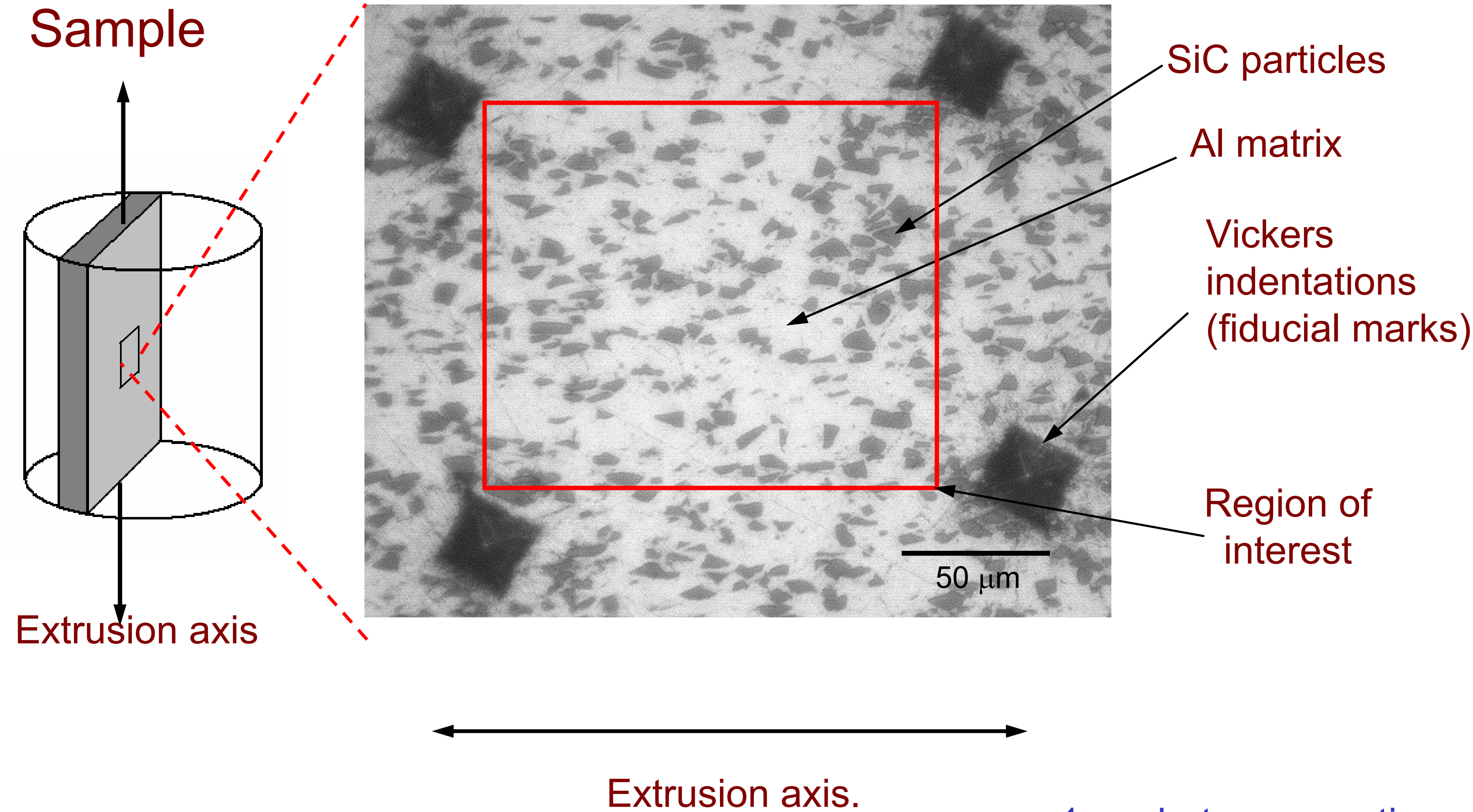

1 μm between sections

3D reconstruction and visualization

2D serial sections stacked on top of each other

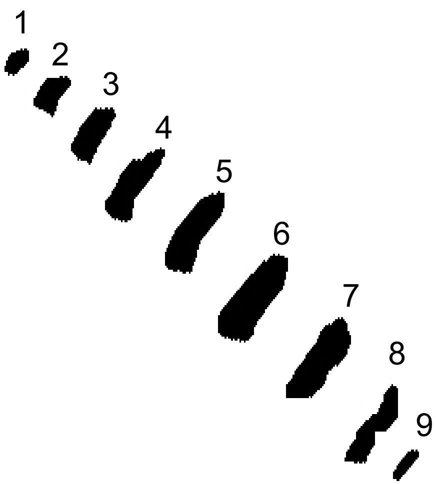

Contour added around the particle in each sections

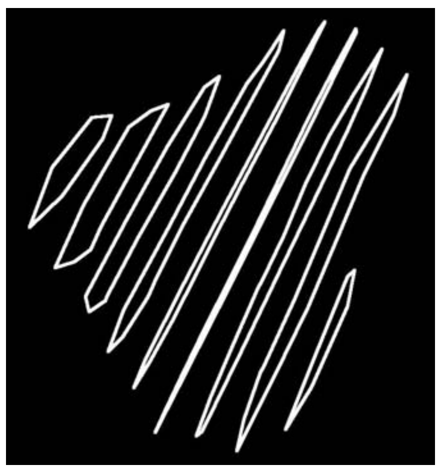

A surfacing process connects the contours to generate 3D object

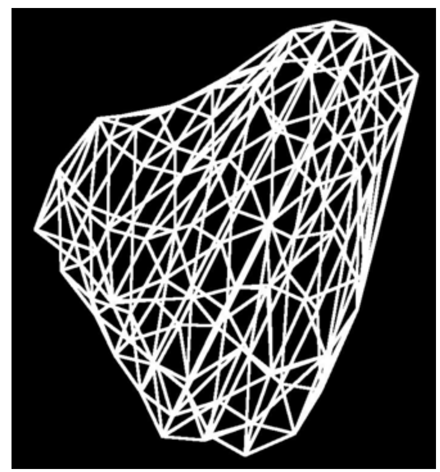

Wire frame view

3D Object

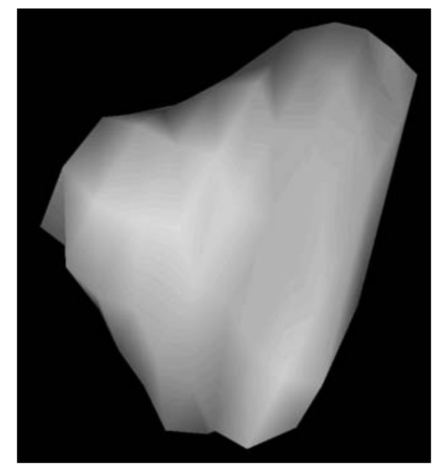

Full texture view

3D Microstructure visualization - 2080/SiC/20$_p$

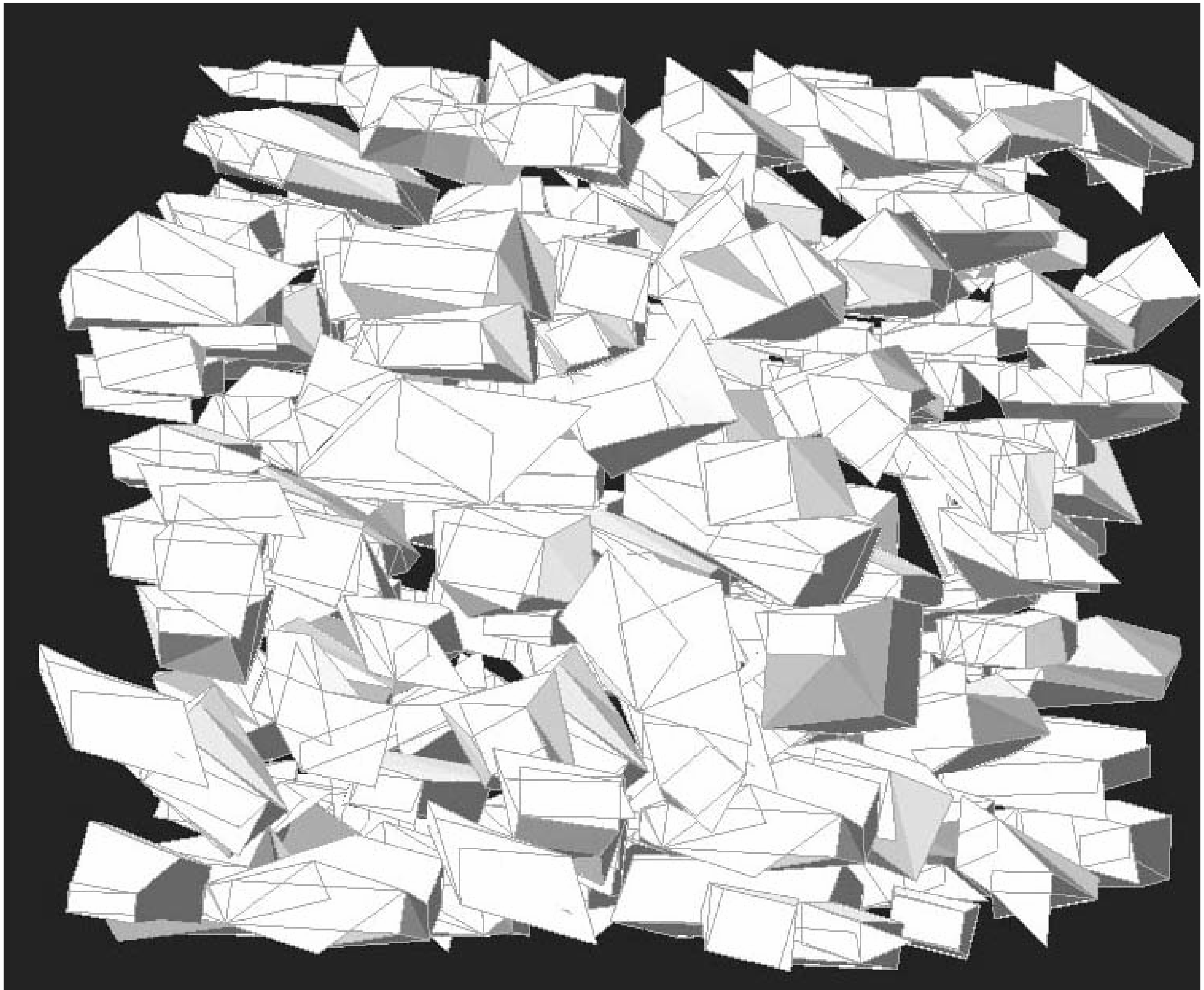

10 μm

Incorporating 3D model into FEM analysis

- The particles are imported into HyperMesh® and the matrix geometry is created.
- The model is then meshed and exported to ABAQUS for analysis

70 Particles

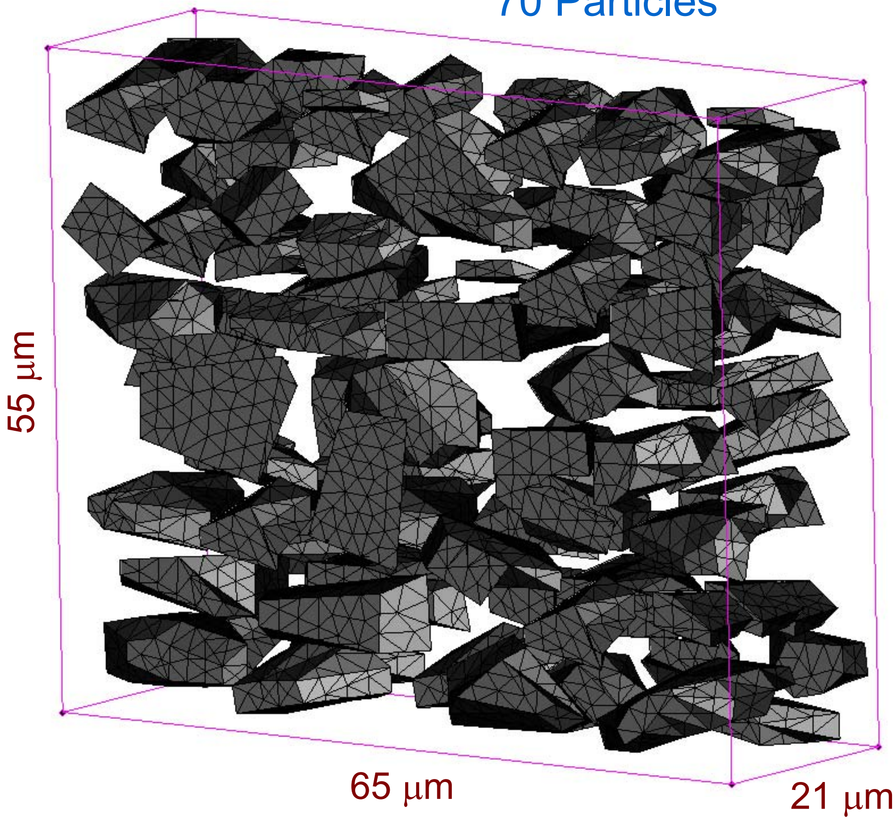

Meshed Model

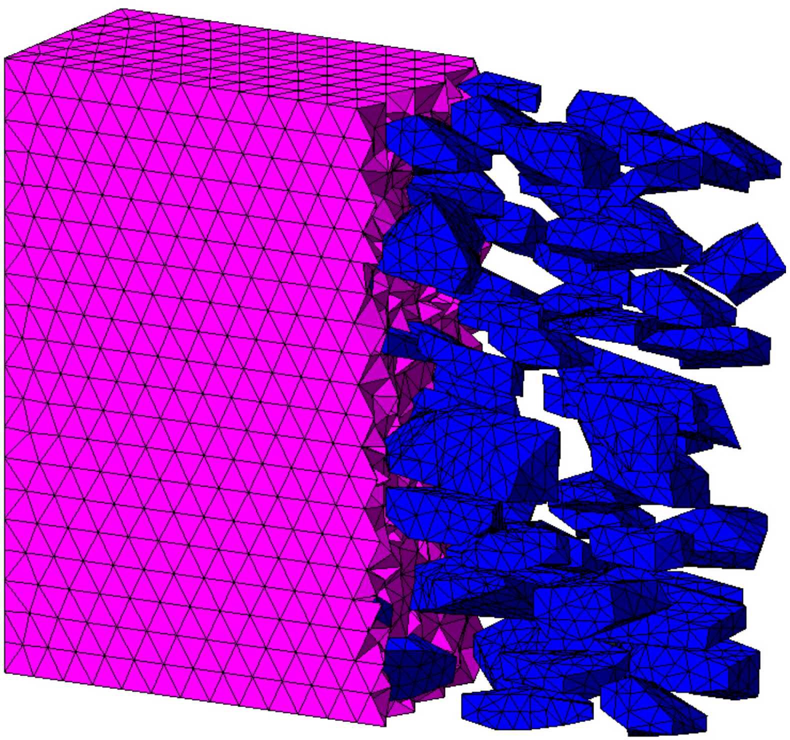

10 node Tetrahedral elements

Effect of model size (Thickness)

3 μm Model

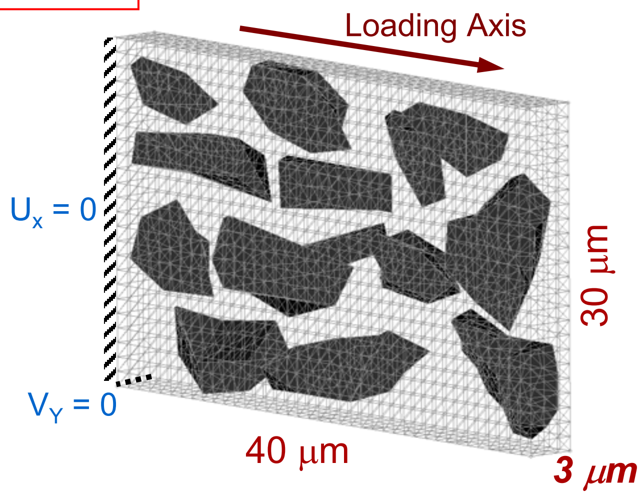

20 μm Model

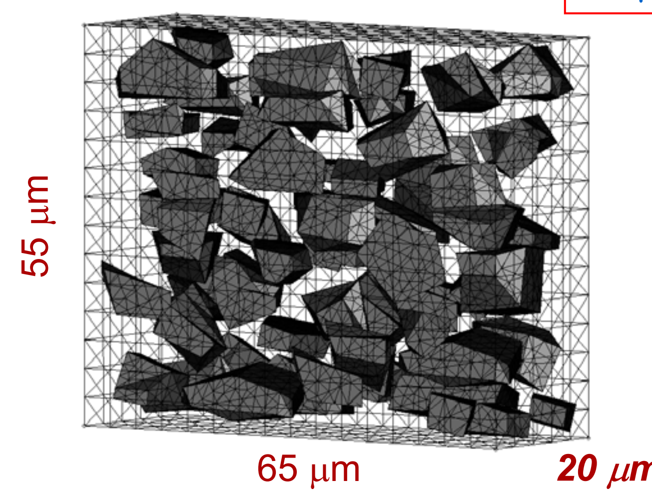

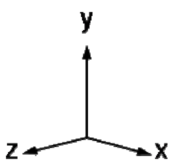

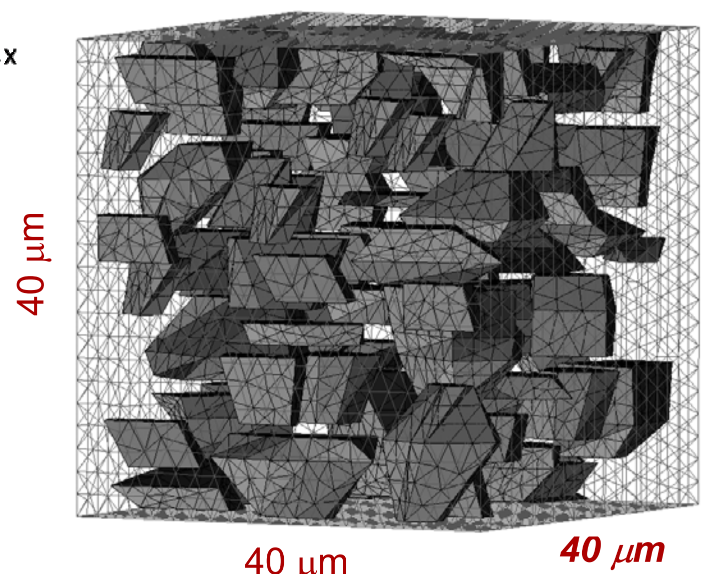

40 μm Model

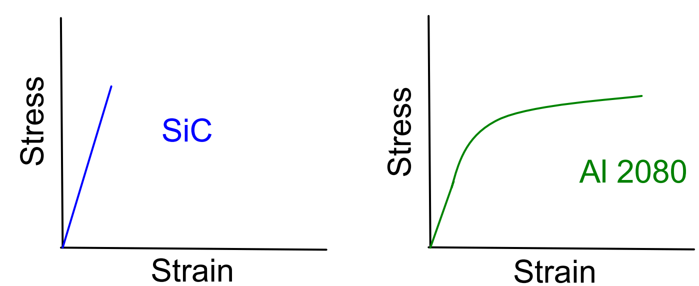

Material	Elastic Modulus (GPa)	Poisson's Ratio
Al	74	0.33
SiC	410	0.19

Effect of model size

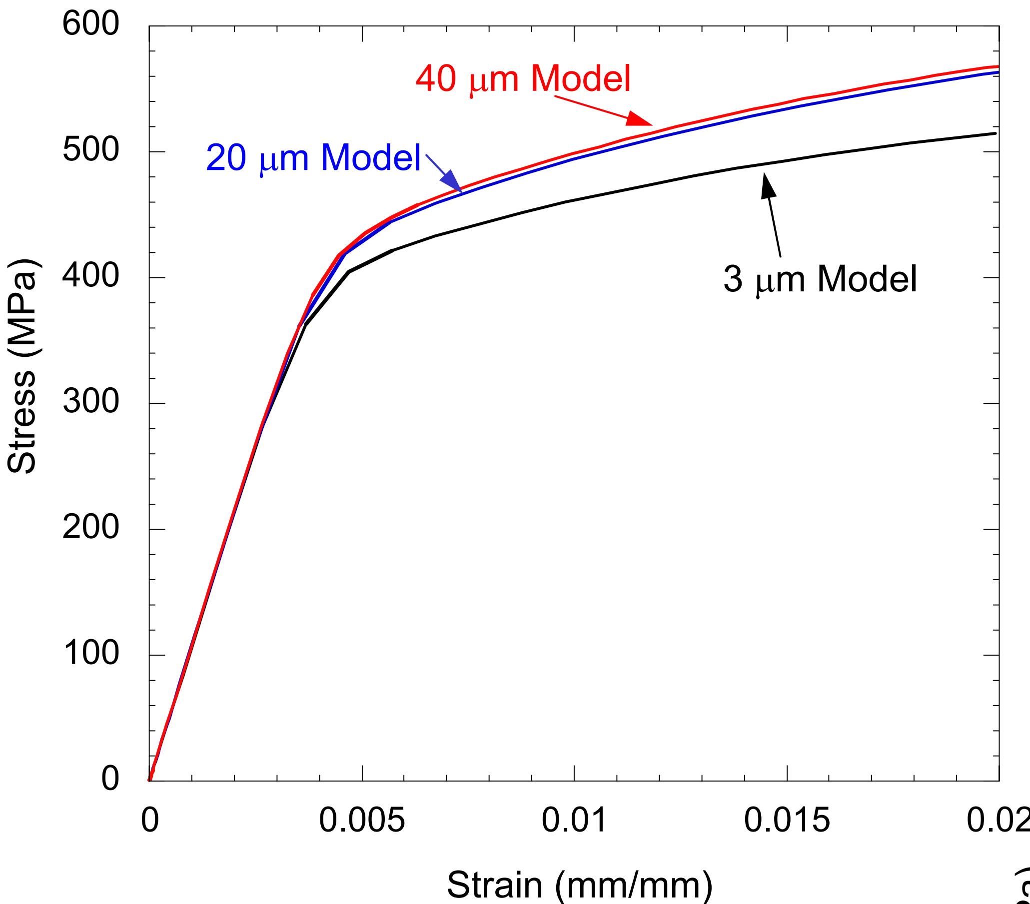

Model	E (GPa)
3 μm	107
20 μm	107.5
40 μm	107.8

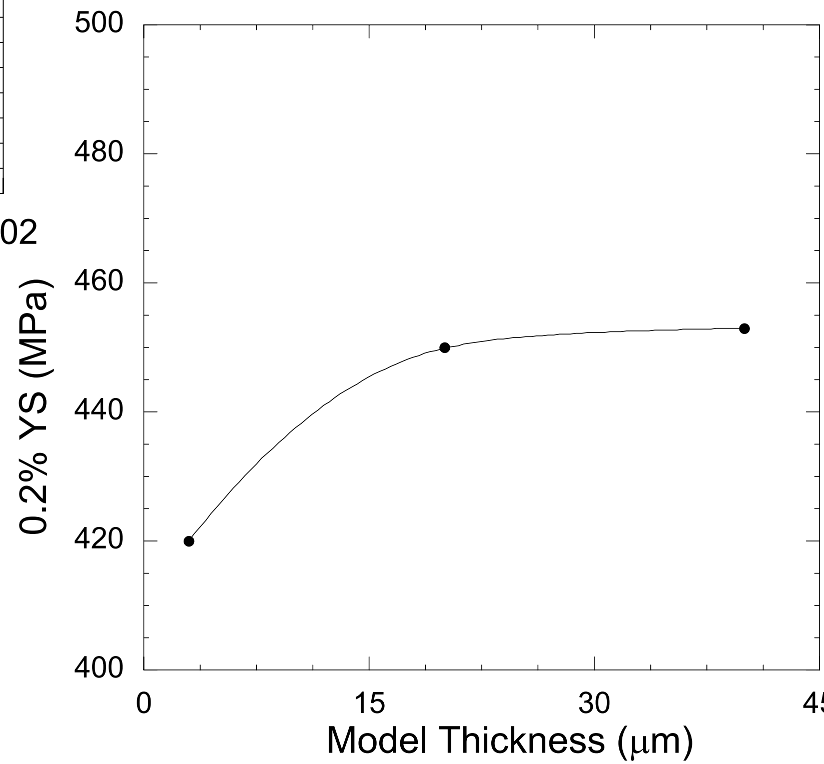

20 μm model was chosen as the representative volume

Microstructure variability

Simulation was carried out on two models created from different regions to validate the approach

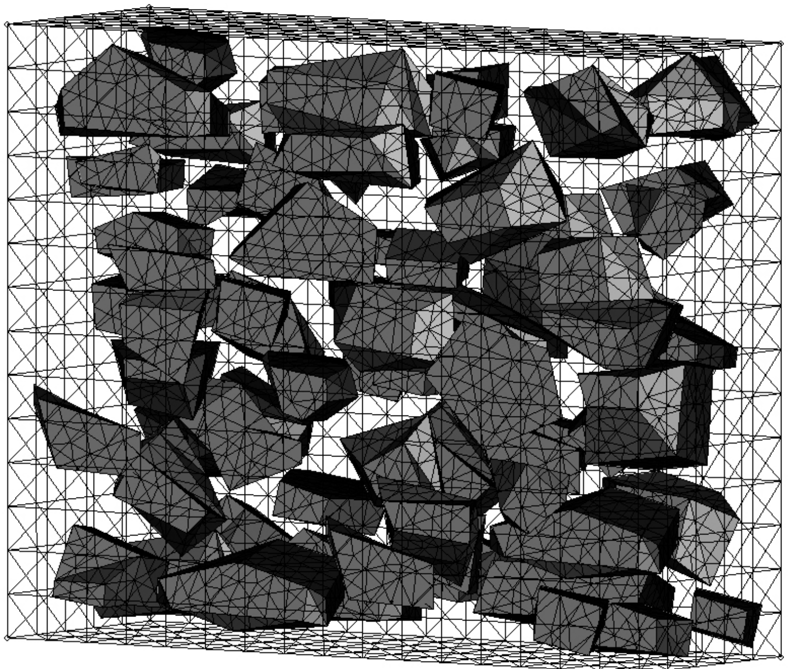

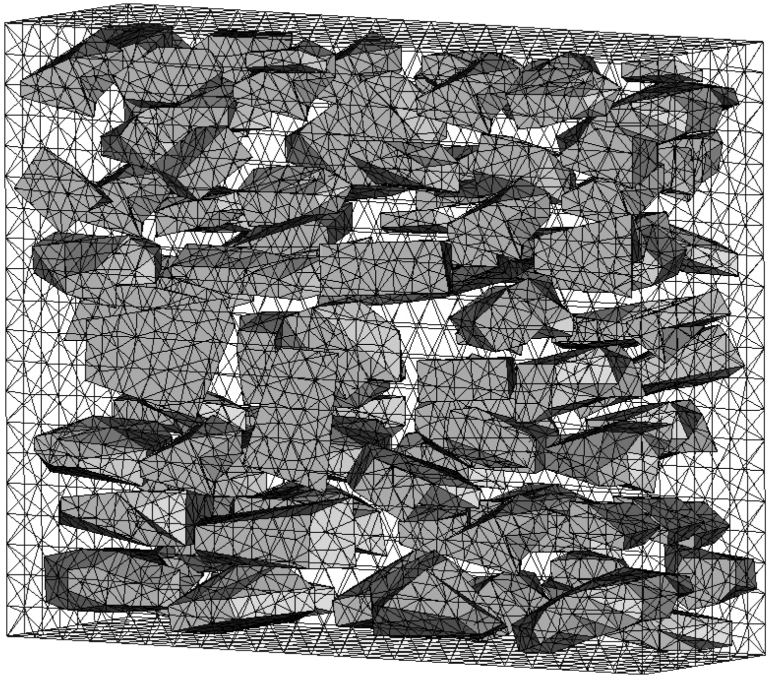

Microstructure variability

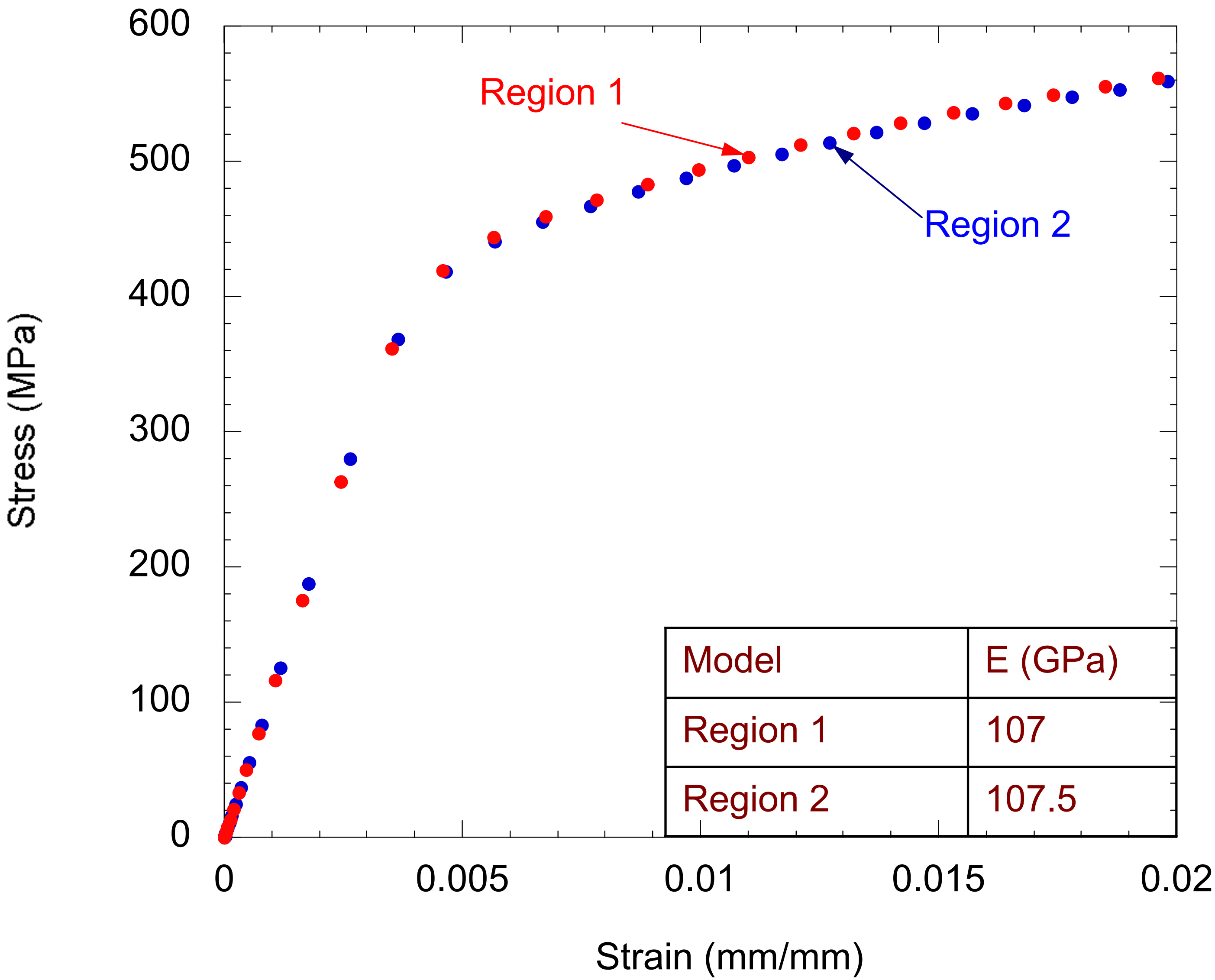

Model	E (GPa)
Region 1	107
Region 2	107.5

Effect of simplifying particle geometry

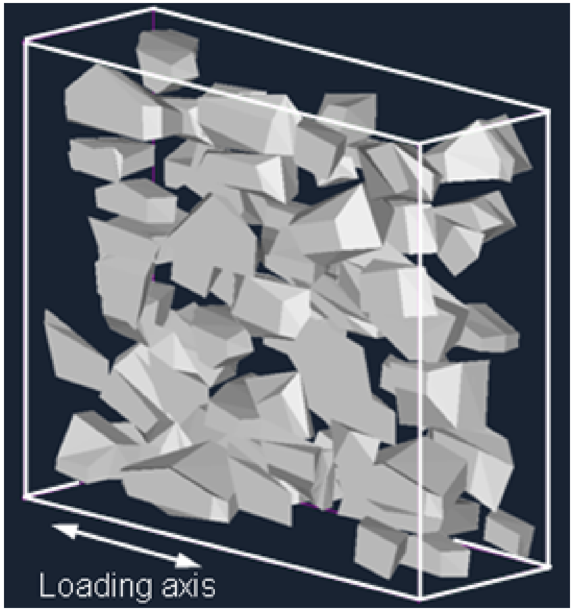

Model	No. of Elements	Hours
3D Ellipsoidal	87323	25
3D Microstructure	89128	26

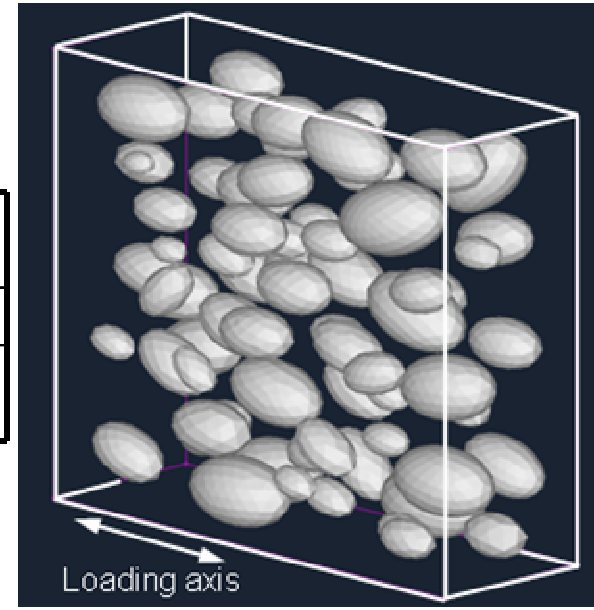

Microstructure

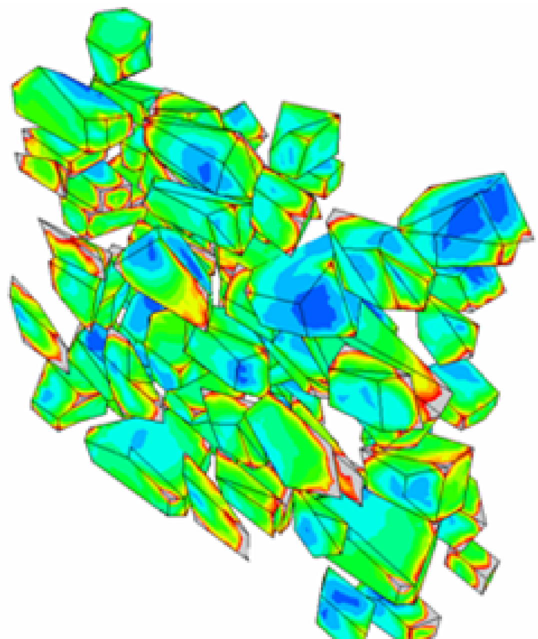

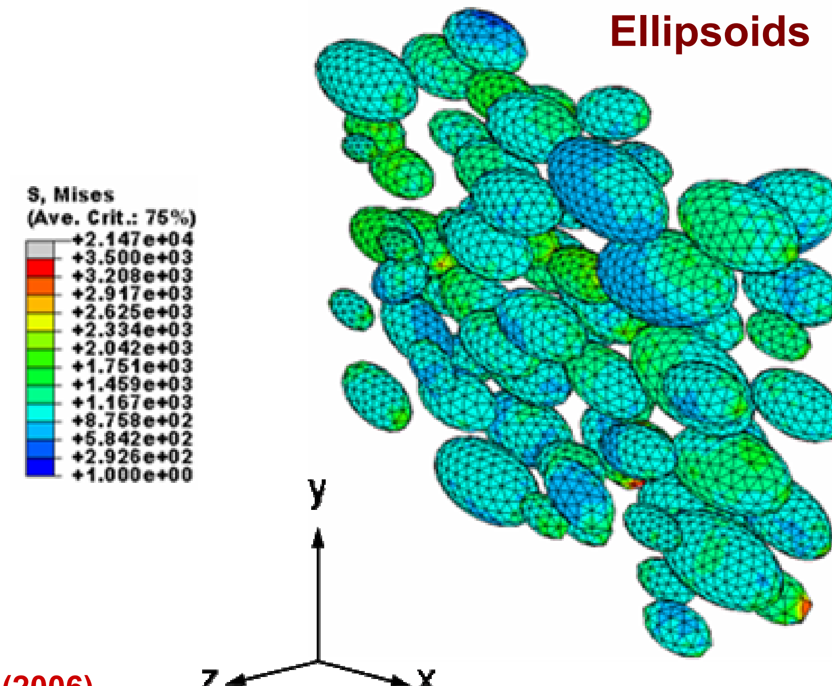

Ellipsoids

N. Chawla, R.S. Sidhu, and V.V. Ganesh, Acta Mater., (2006).
N. Chawla and K.K. Chawla, J. Mater. Sci. – 40th Ann. (1966-2006), (2006).

Comparison of microstructure-based model with conventional models and experiment

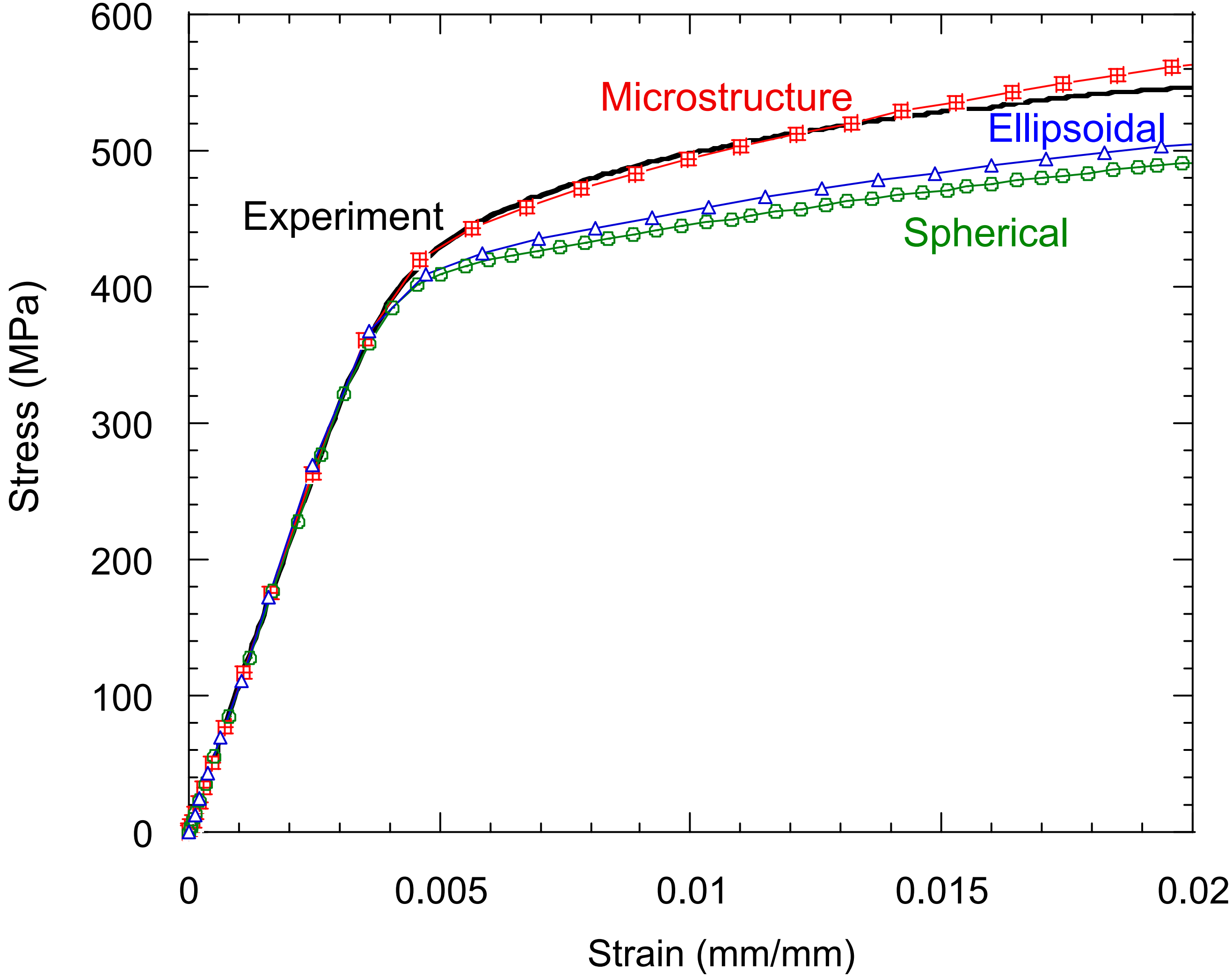

N. Chawla, R.S. Sidhu, and V.V. Ganesh, Acta Mater., (2006).

N. Chawla and K.K. Chawla, J. Mater. Sci. – 40th Ann. (1966-2006), (2006).

Experimental verification of internal strain/stress by neutron diffraction

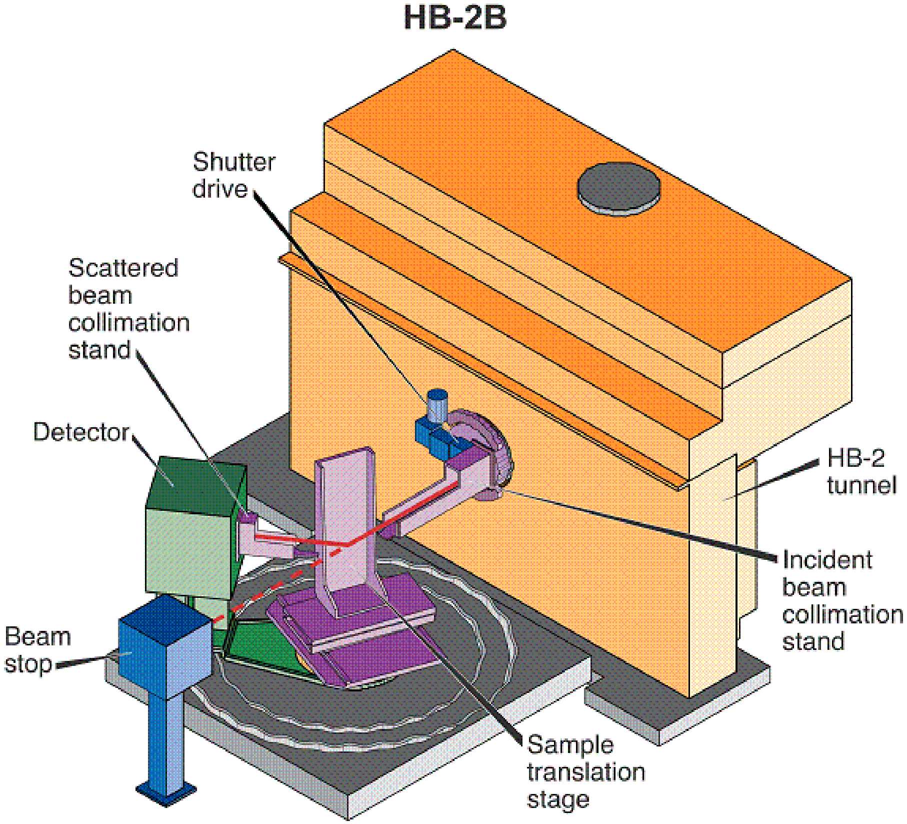

http://neutrons.ornl.gov/

Monochrometer: 1.452, 1.731, 1.886, 2.275 Å

Detector Angel: 30-150^{o}

Detection System: 7 Position-Sensitive Detectors

Detector Resolution: 1.8 mm

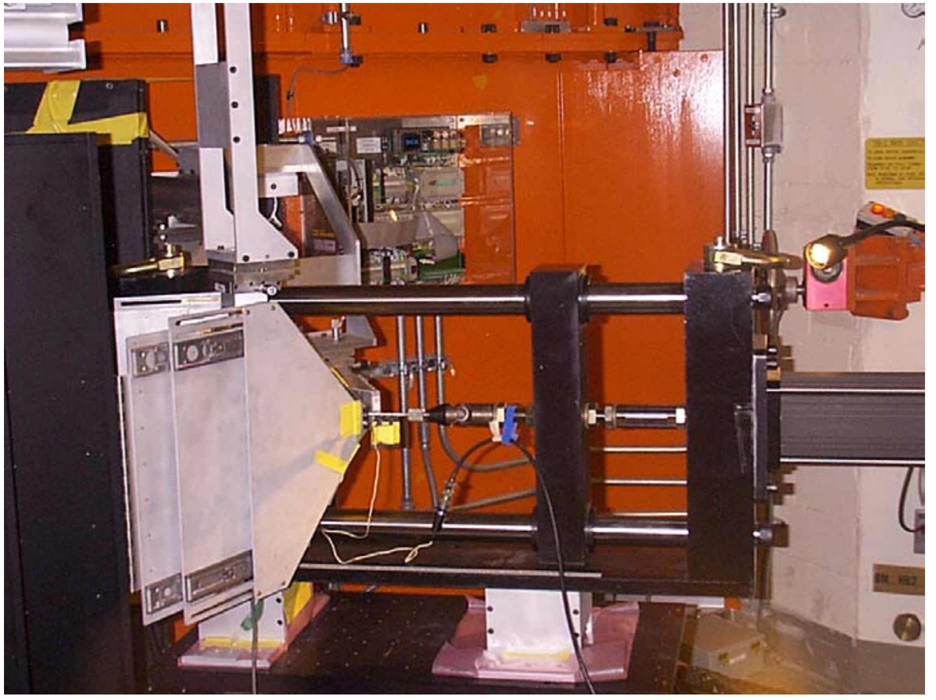

Measurement of internal strains during tensile test

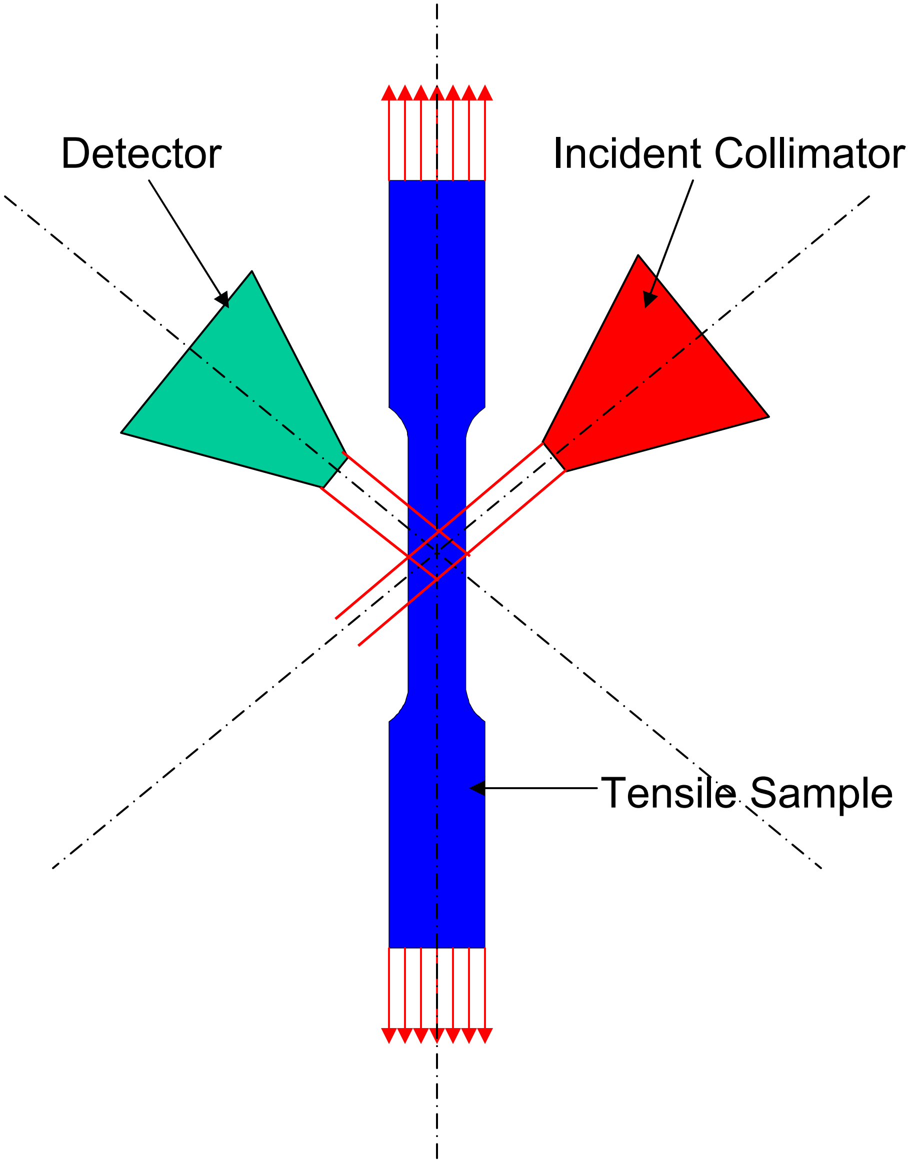

Neutron Diffraction for Longitudinal Internal Strain Measurement

Diffraction Peak: Al (311), SiC (116)

Monochrometer: 1.729567 Å

Gauge Volume: 5×5×5 mm

Displacement Control Rate: 0.0005 mm/s

Displacement Step Size: 0.02 mm

Diffraction Acquisition Time: Al-8 minutes, SiC-4 minutes

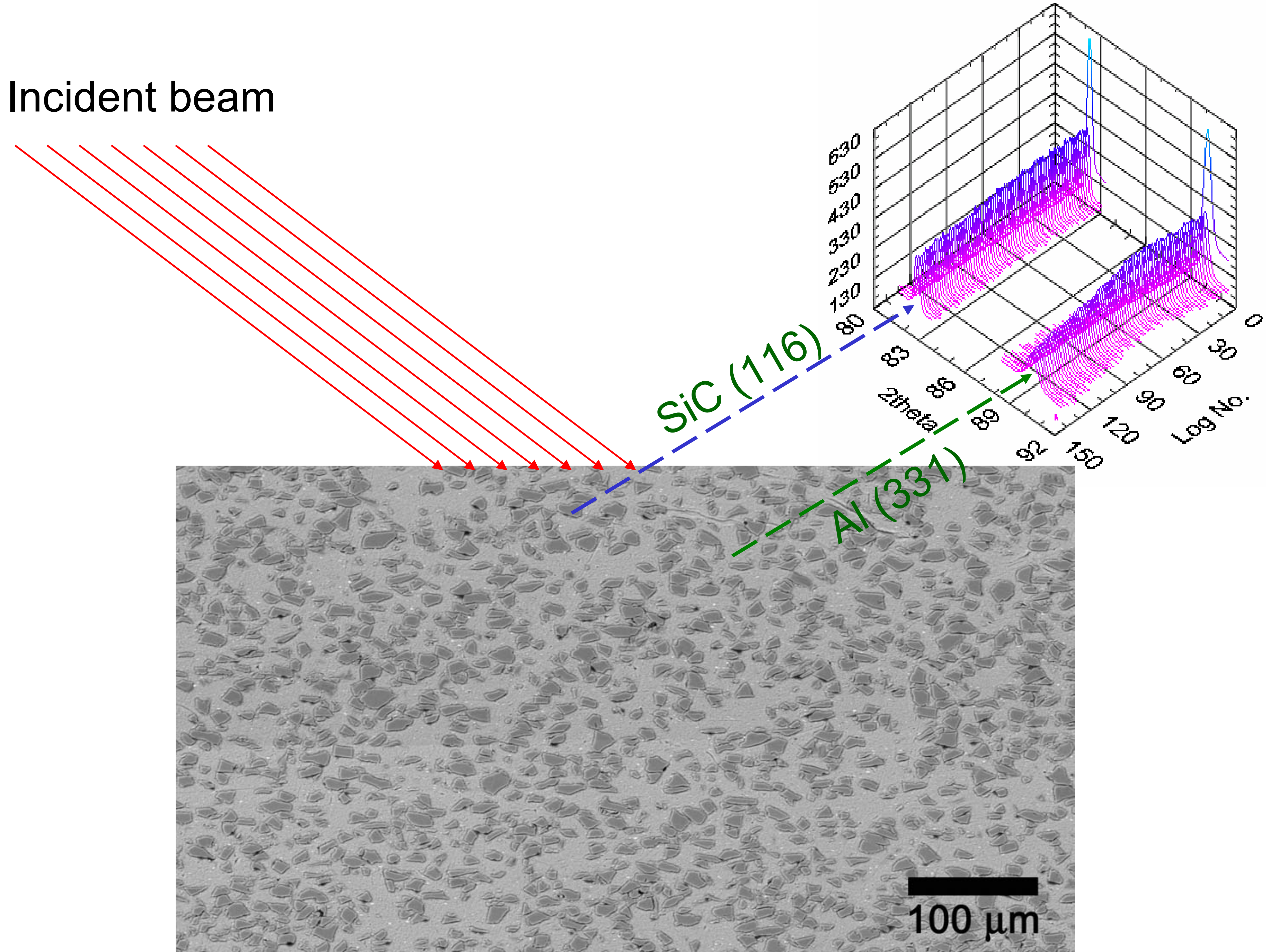

Incident beam
SiC (116)
Al (331)
630
530
430
330
230
130
80
83
86
89
92
2theta
0
30
60
90
120
150
Log No.
100 μm

Comparison of global stress and internal stress during tensile testing

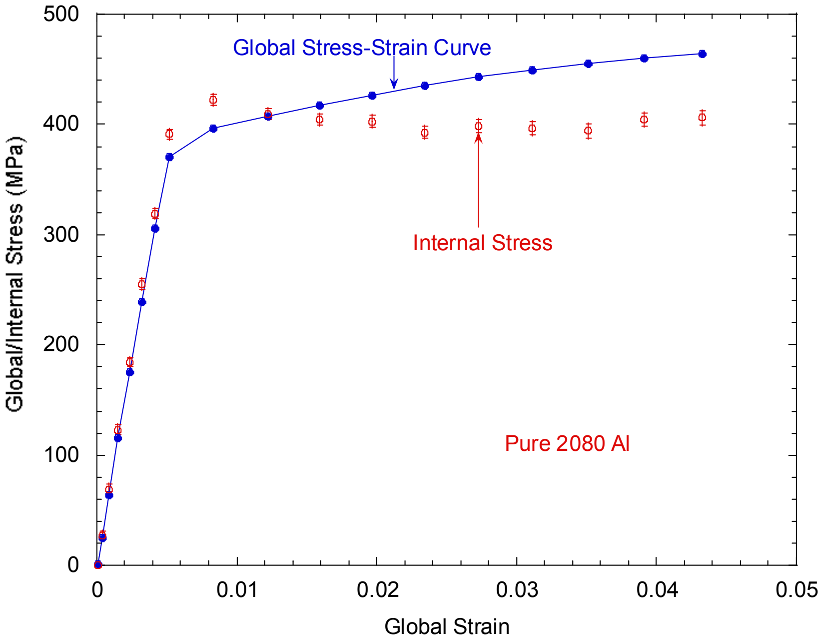

Internal stress of Al matrix and SiC particle was measured by neutron diffraction.

Strains were calculated by changes in lattice spacing during tensile testing.

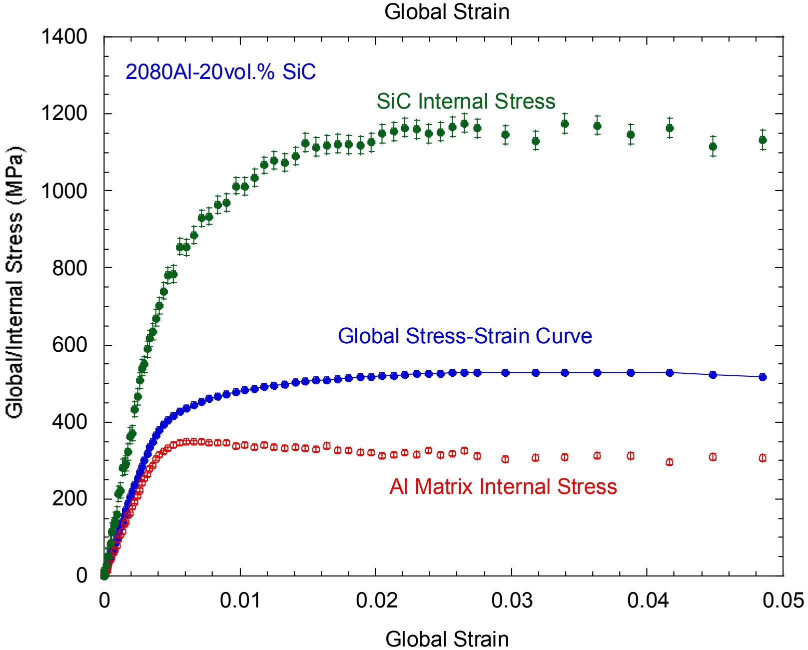

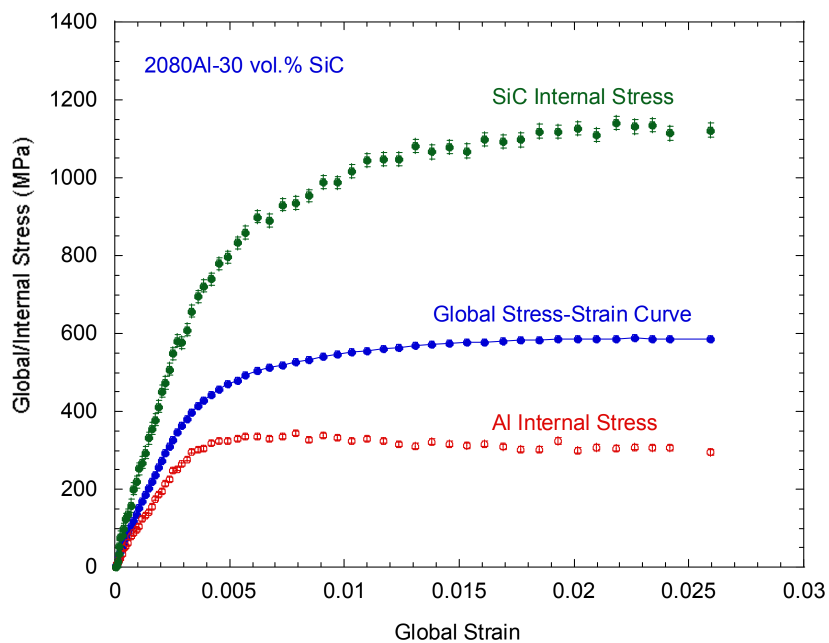

Comparison of microstructure-based FEM predictions of stress/strain partitioning with neutron diffraction measurements

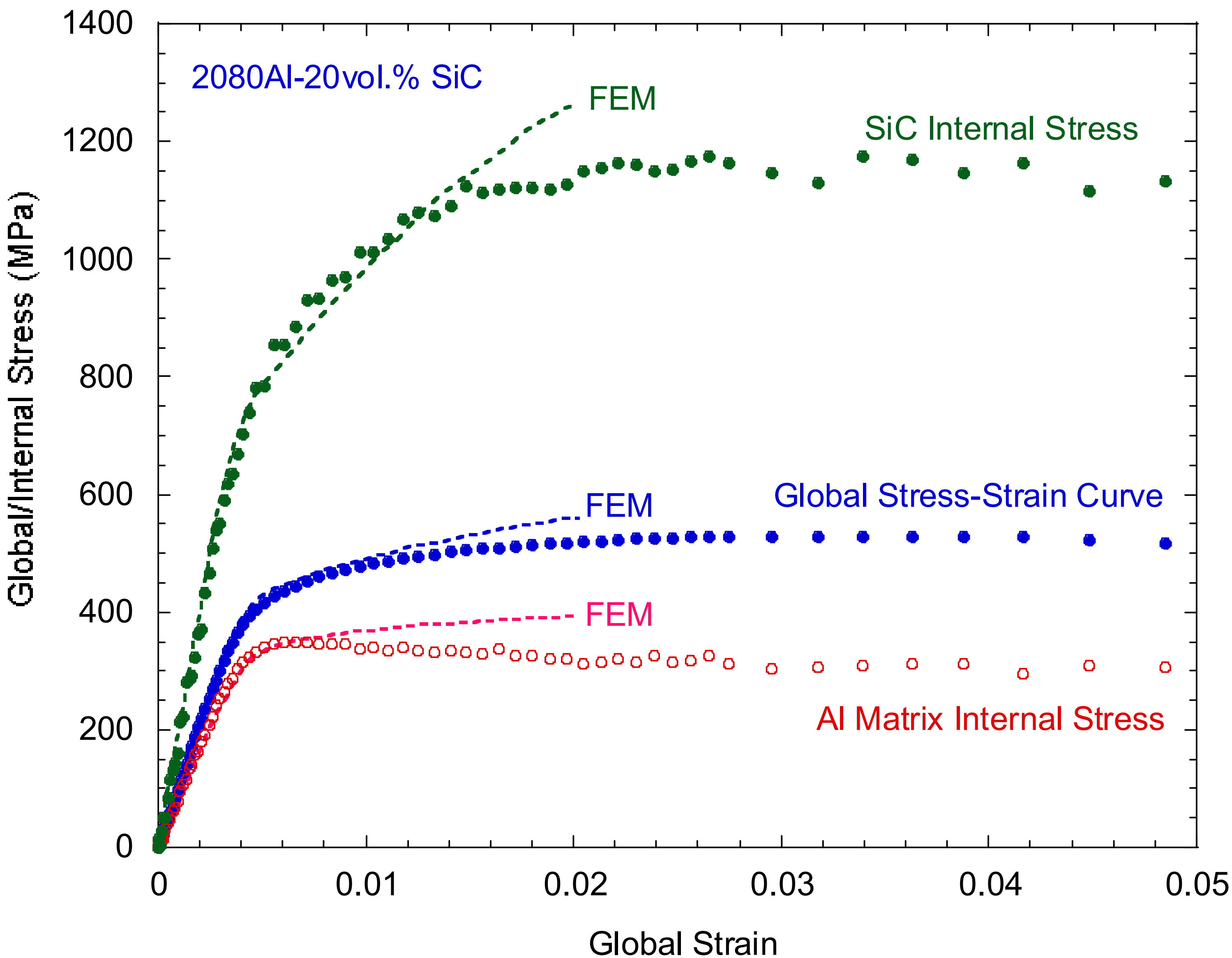

Modeling crack growth in particle reinforced composites

Al/SiCp system

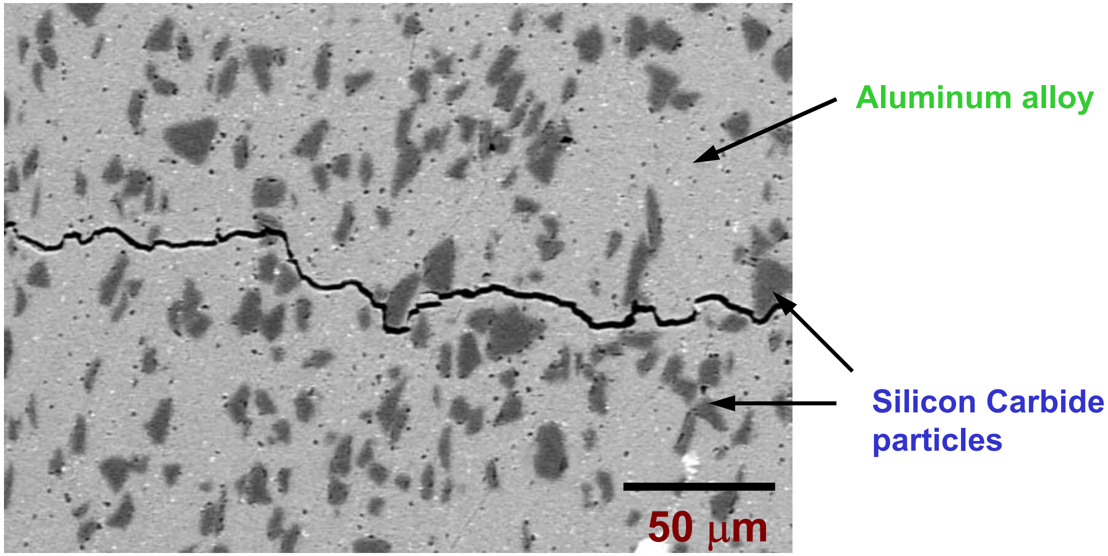

- FRANC2D/L* was used to model crack growth
- Crack path was not known in advance, hence re-meshing method was used
- Fracture calculations using **L**inear **E**lastic **F**racture **M**echanics (LEFM) principles
  - Stress Intensity Factors that govern the fracture process were calculated using *Modified crack closure method*
  - *Max. Circumferential Tensile Stress theory* was used to determine the crack propagation direction

***Mark James and Daniel Swenson, (1998), http://www.mne.ksu.edu/~franc2d/**

Numerical model description

- Plane stress
- Elements = 18,000; Nodes = 47,000

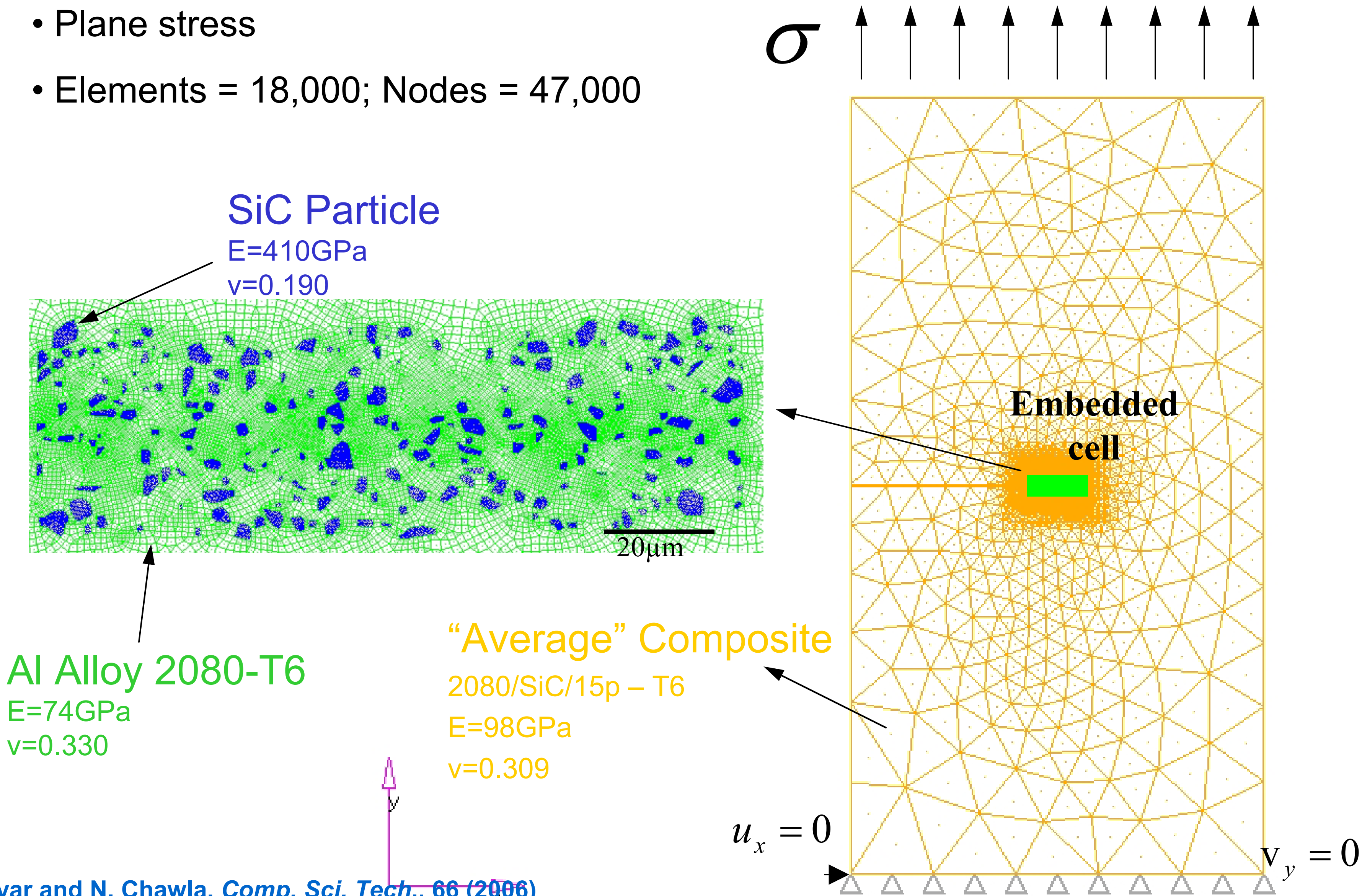

A. Ayyar and N. Chawla, *Comp. Sci. Tech.*, 66 (2006)

Simulated crack paths in models with clustered particle distribution

Crack growth direction

$$D_{50}^{Al} = 33\mu m \qquad D_{50}^{SiC} = 5\mu m$$

Ratio = 6.6

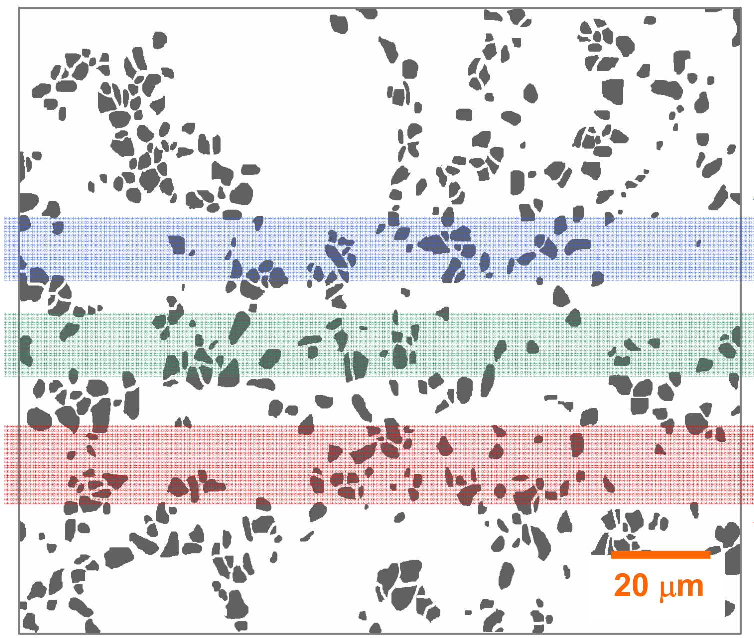

Embedded cells

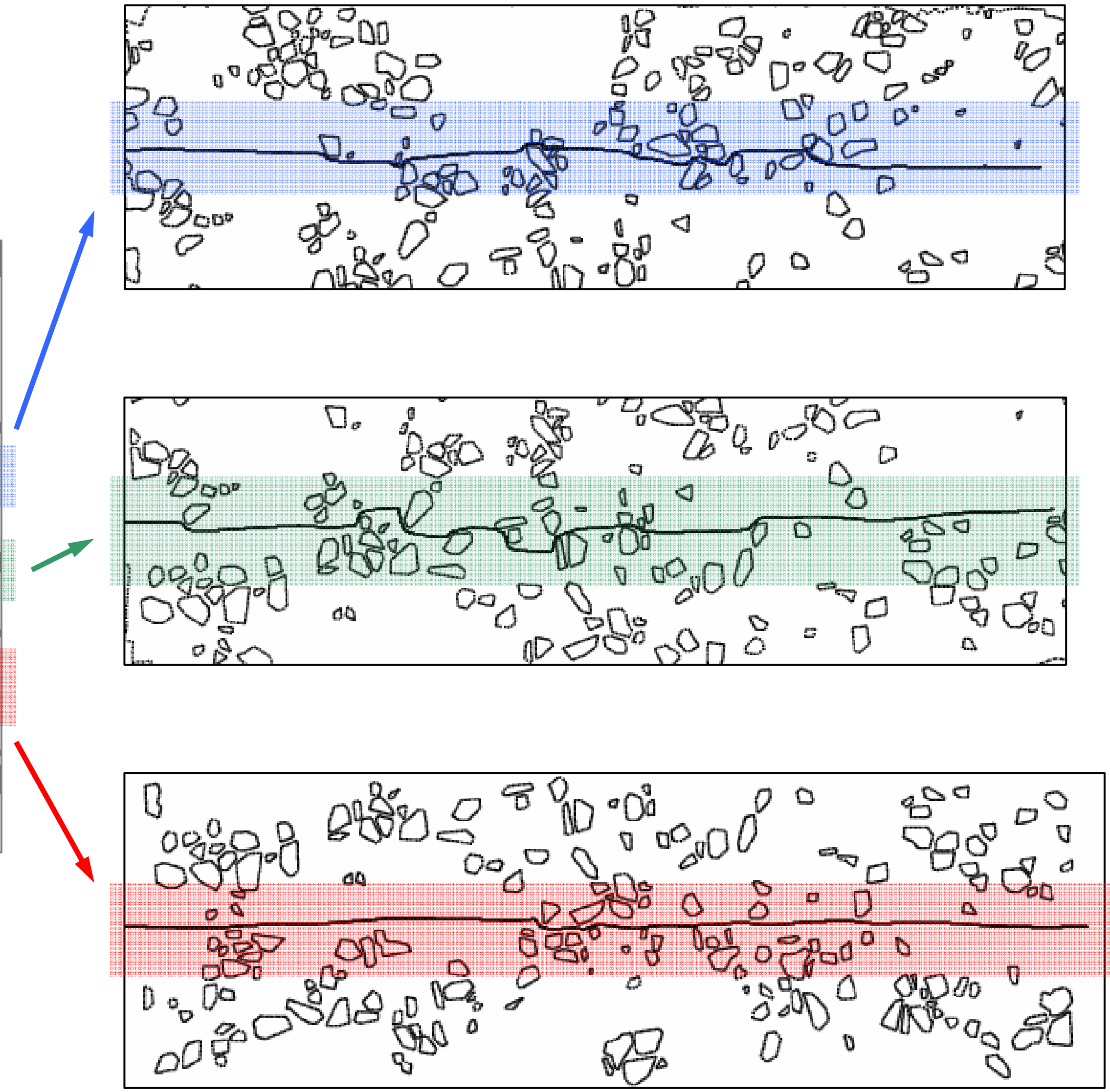

A. Ayyar and N. Chawla, *Comp. Sci. Tech.*, 66 (2006)

Fatigue crack growth mechanisms at Low/High R-Ratio

Before Crack Growth | **After Crack Growth**

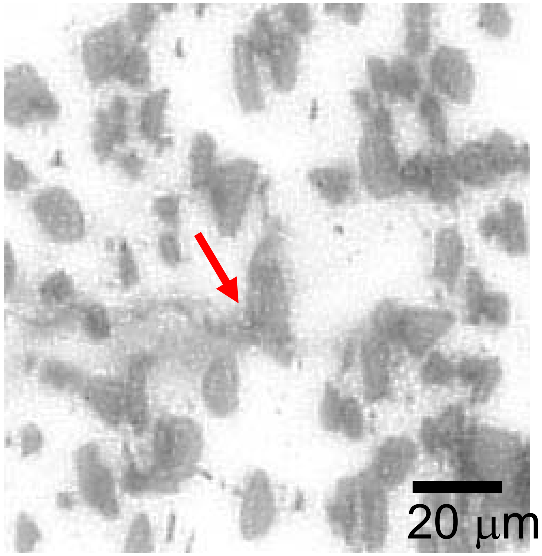

R = 0.1

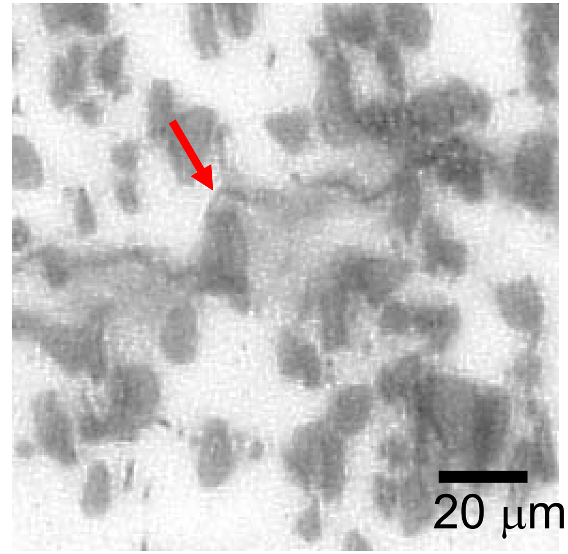

Crack growth is observed around the SiC particles.

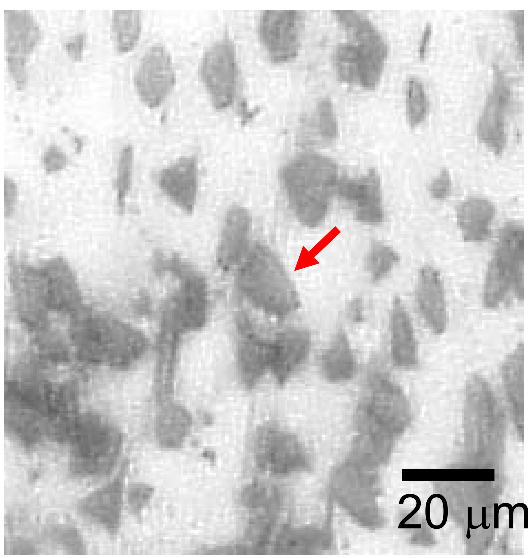

R = 0.8

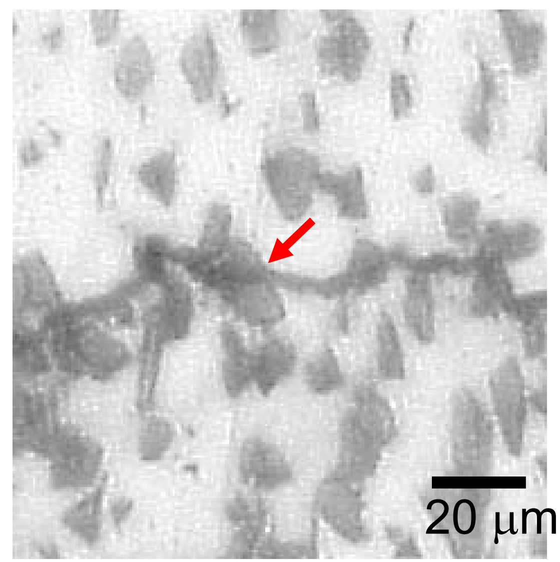

Crack growth is observed through the SiC particles.

Ganesh and Chawla, (2004)

Motivation for modeling reinforcement particle fracture

- Reinforcement particles do not posses infinite strength.
- Regions around a crack-tip are at a high stress state. How does this high stress influence the load bearing capabilities of the particle?
- When particles fracture, how do they influence the crack path and the crack-tip driving force?

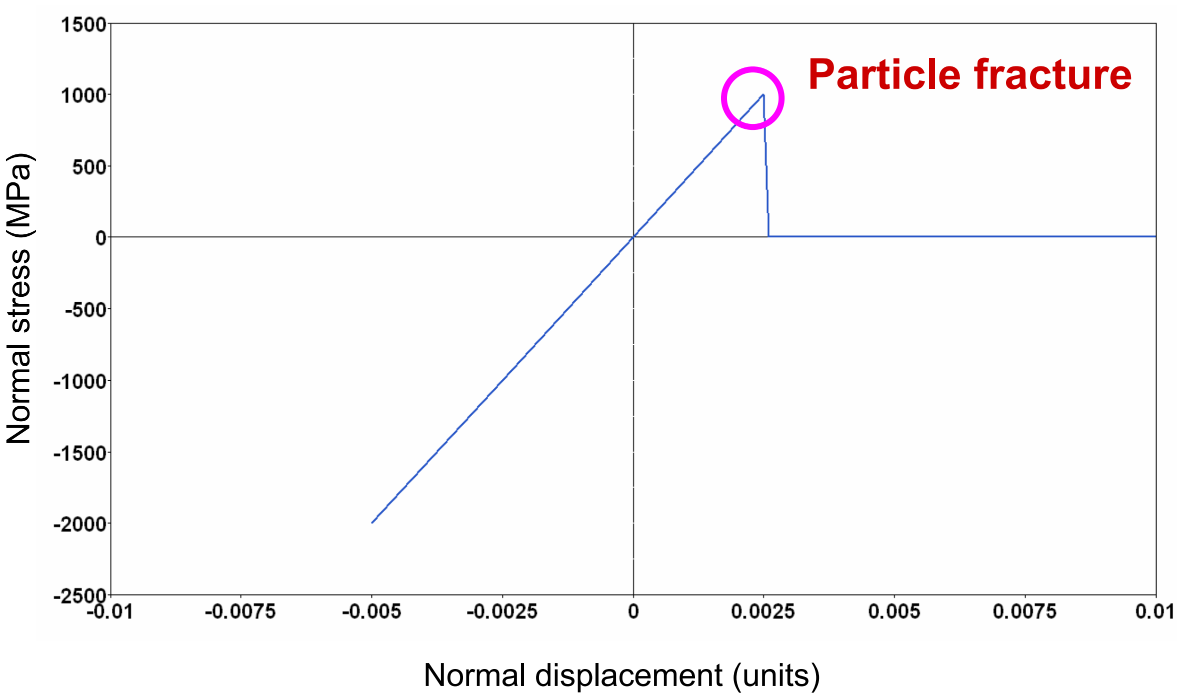

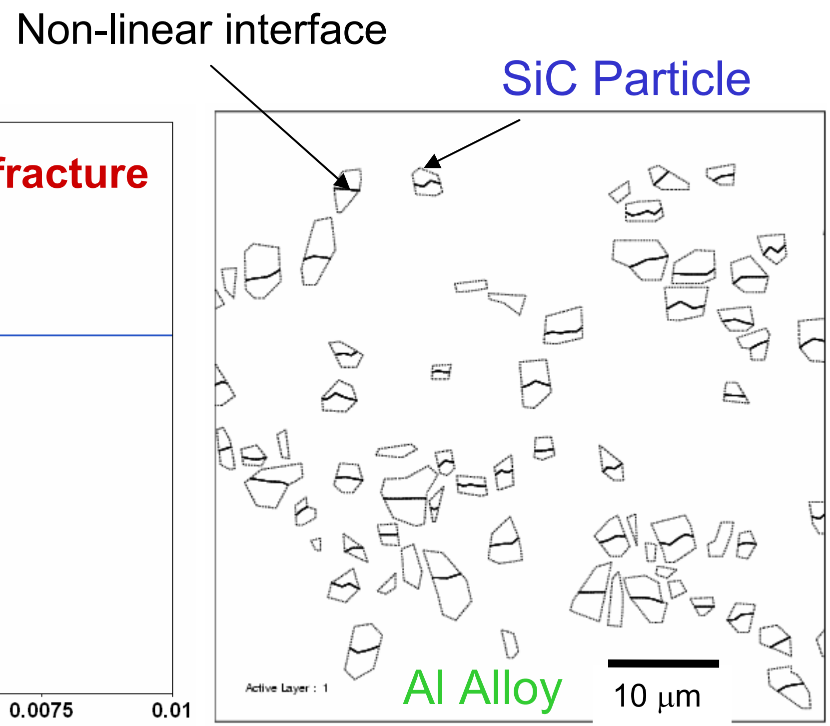

Crack propagation with particle fracture

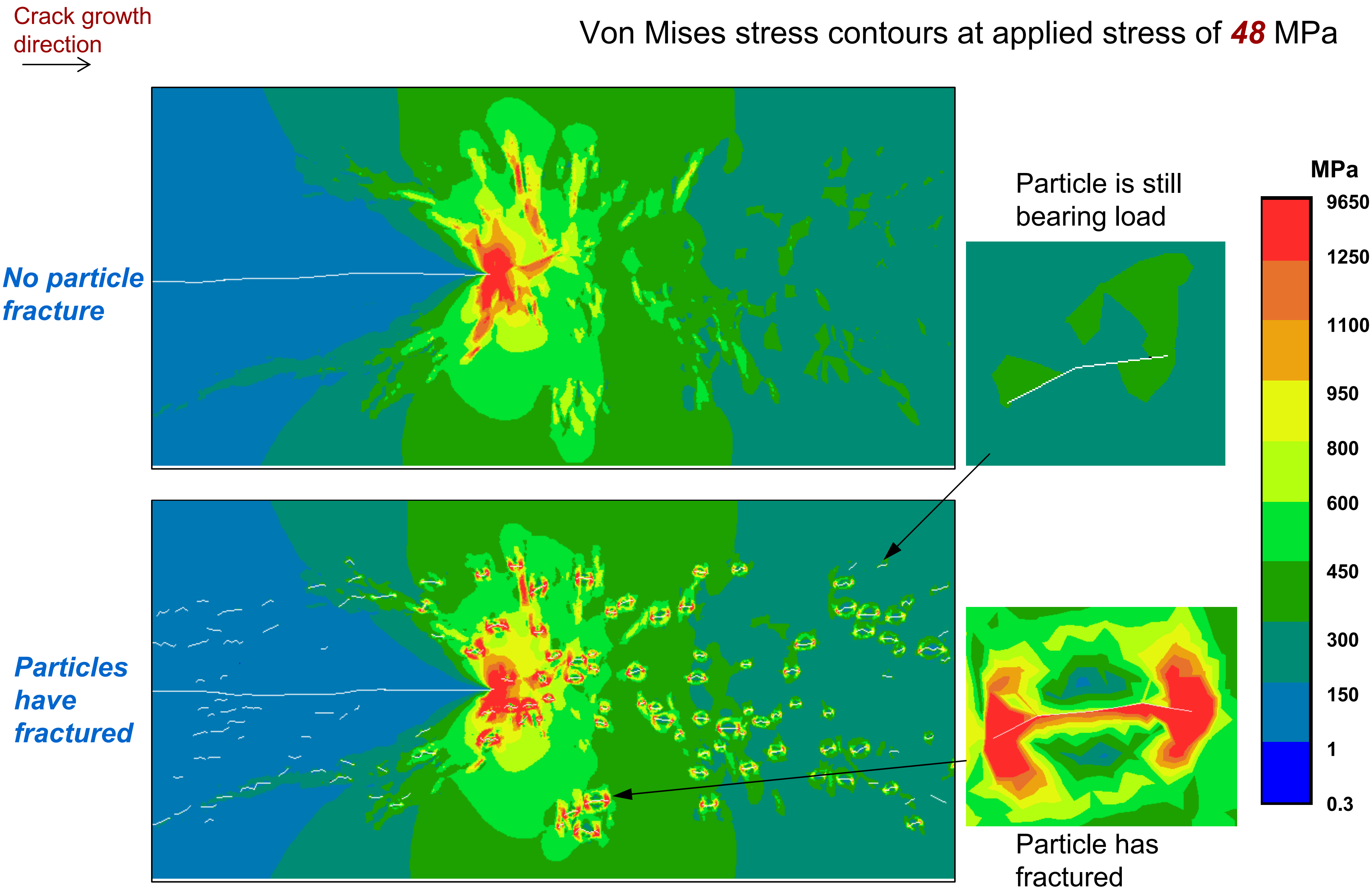

Von Mises stress contours for varying loads

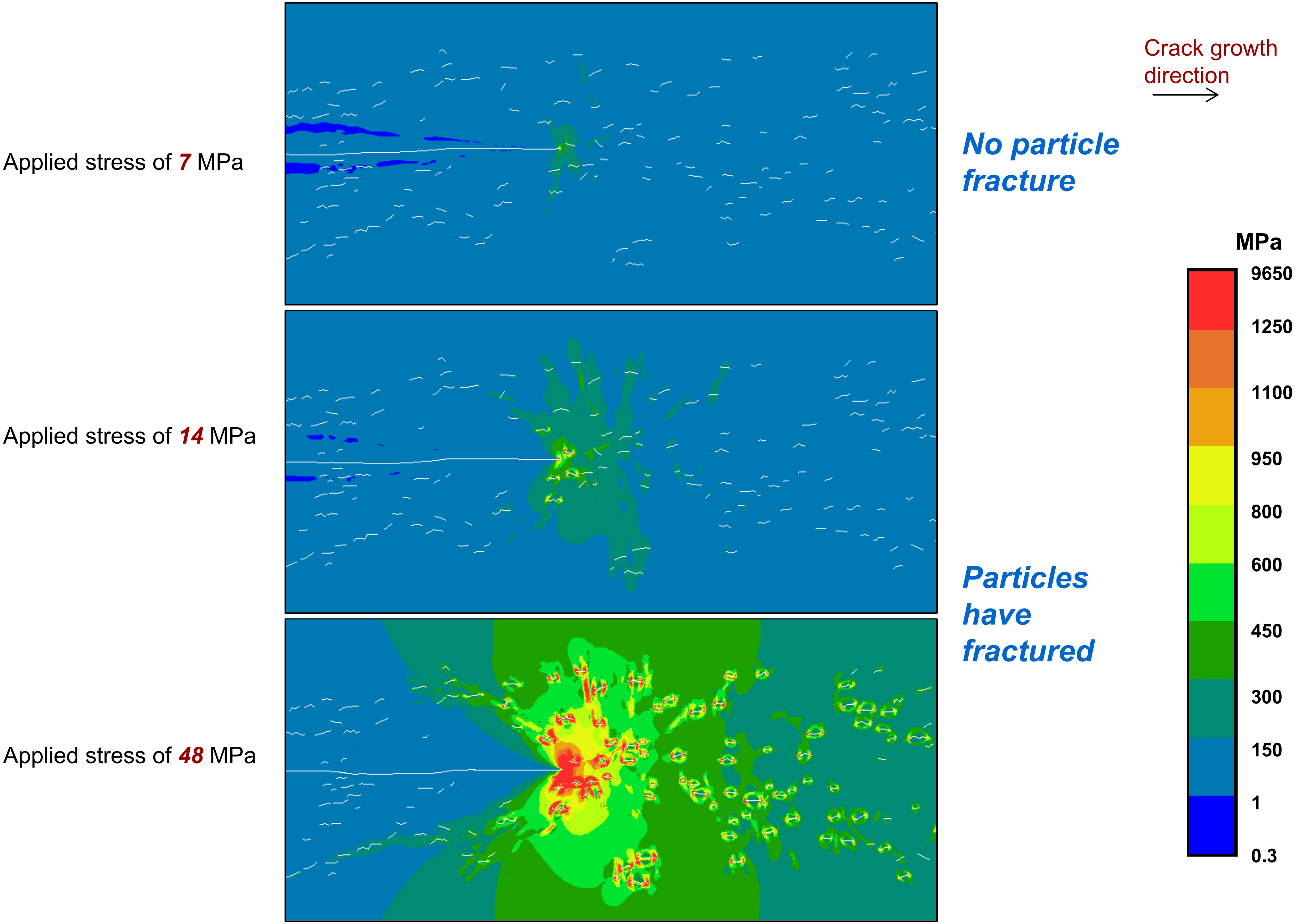

Influence of particle fracture on crack trajectory

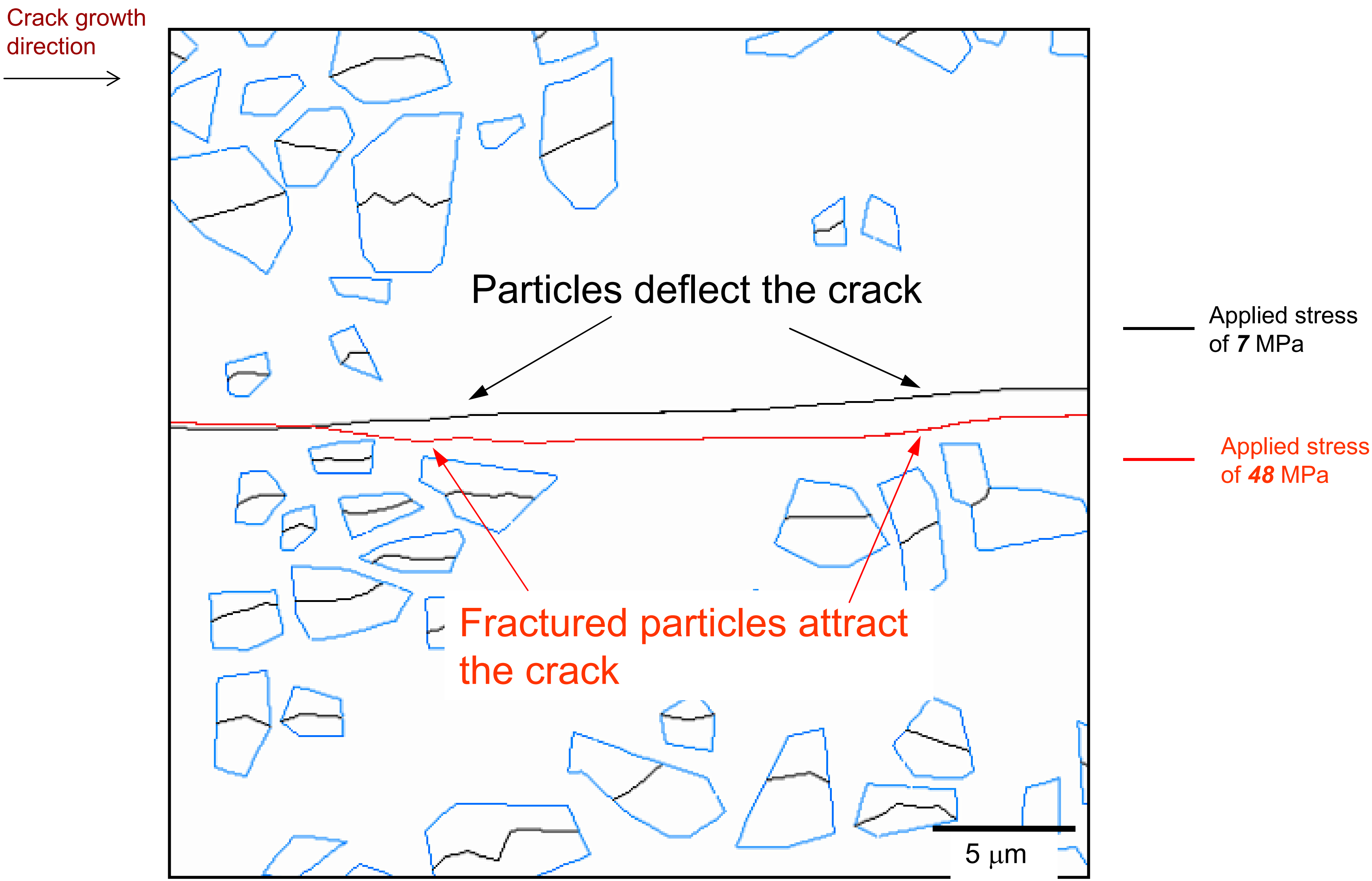

Normalized SIF vs. crack length

Applied stress of ***7*** MPa

Applied stress of ***14*** MPa

Applied stress of ***48*** MPa

$$\frac{k_I(AlSiC)}{k_I(cp)}$$

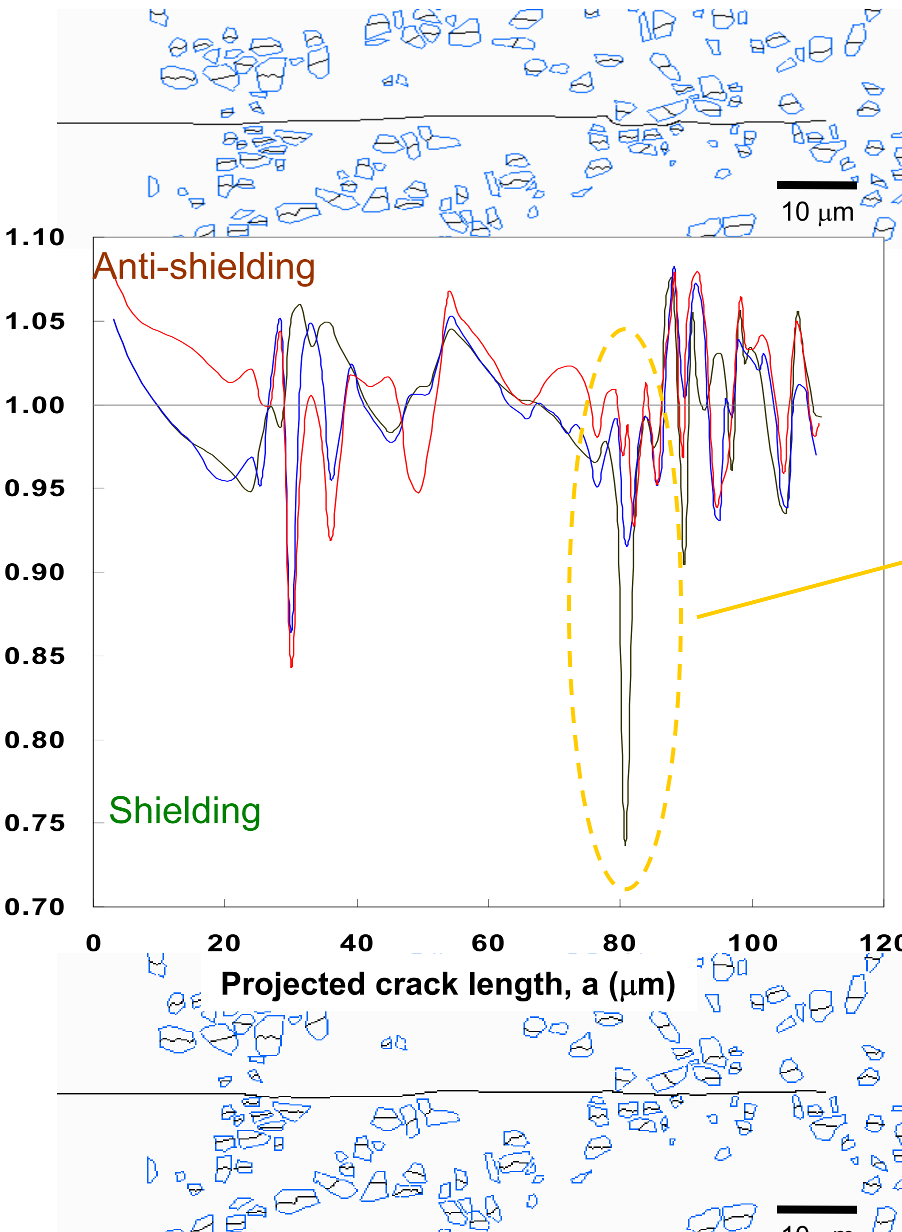

Crack growth direction

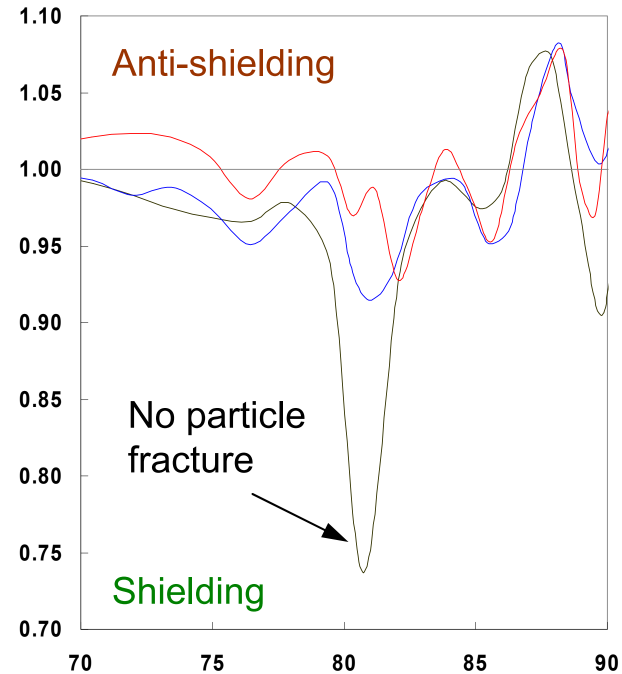

Particle fracture influences the crack-tip driving force

Ongoing research

- Modeling particle (SiC) fracture in 3D models
- Clustering analysis in 3D
- Modeling crack growth in 3D

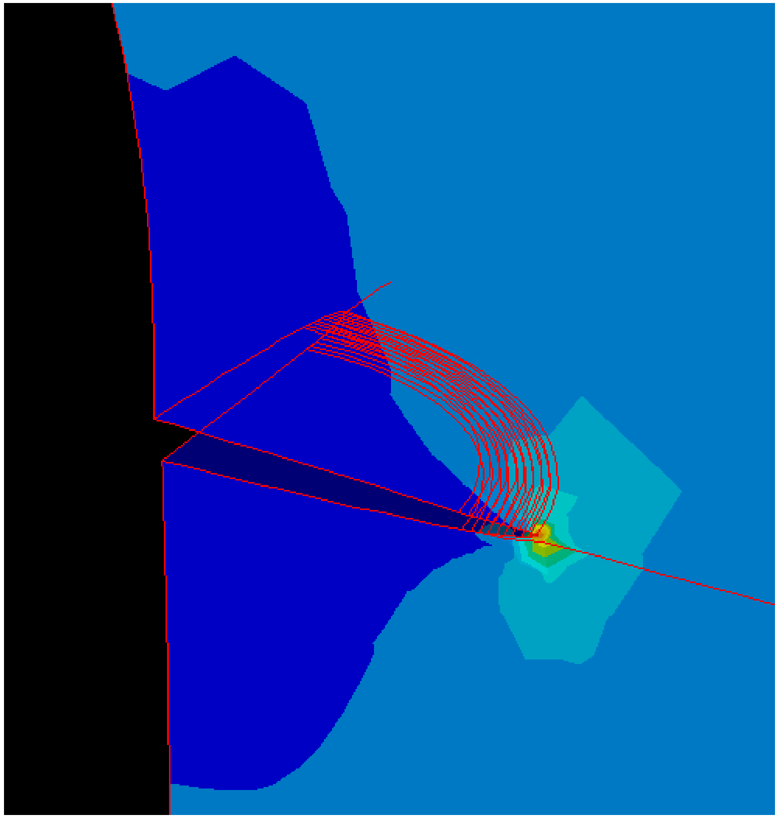

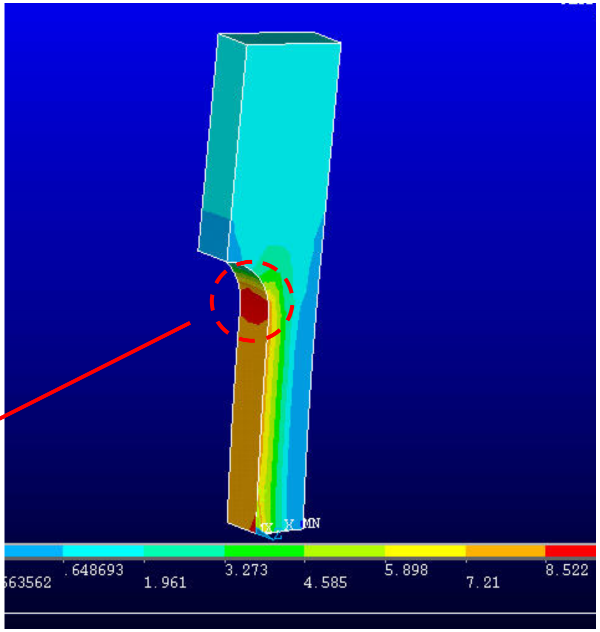

http://www.cfg.cornell.edu/index.htm

Acknowledgments

- Postdocs: X. Deng (Kennametal) and J.J. Williams
- Graduate Students: R. Saha, B. Wunsch (MIT), and V.V. Ganesh (Intel)
- Office of Naval Research (ONR)
  - N00014-01-1-0694 (Program Manager: A.K. Vasudevan)
- High Temperature Materials Laboratory User Program (ORNL)
- M. James and D. Swenson, "FRANC2D/L: A Crack Propagation Simulator for Plane Layered Structures," available from http://www.mne.ksu.edu/~franc2d/.

E-mail: nchawla@asu.edu
www.eas.asu.edu/~cme/cme-faculty/chawla